AD-A151 730 THE THEORETICAL RESPONSE OF A VERTICAL LINE ARRAY TO WIND-GENERATED NOISE IN SHALLOW WATER(U) SACLANT ASW RESEARCH CENTRE LA SPEZIA (ITALY) R M HAMSON 15 DEC 84 1/1

UNCLASSIFIED SACLANTCEN-SR-82 F/G 20/1 NL

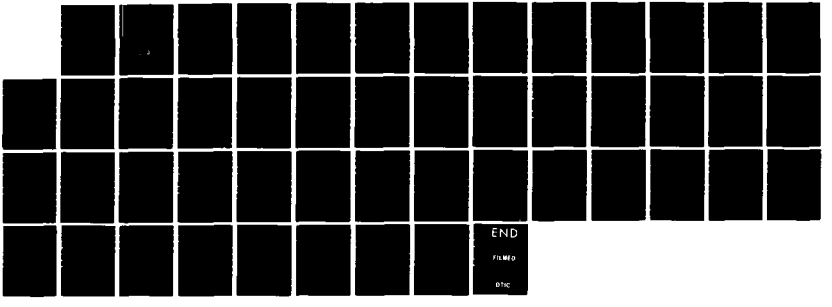

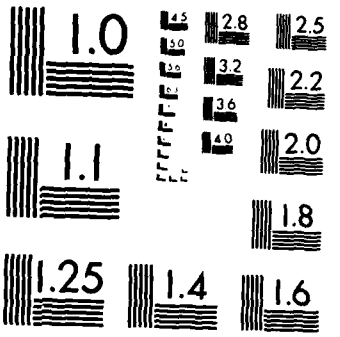

SACLANTCEN Report SR - 82

SACLANTCEN Report SR - 82

SACLANTCEN Report SR - **82**

SACLANT ASW RESEARCH CENTRE REPORT

THE THEORETICAL RESPONSE OF A VERTICAL LINE ARRAY TO WIND-GENERATED NOISE IN SHALLOW WATER

by
Rachel M. HAMSON

15 DECEMBER 1984

NORTH ATLANTIC TREATY ORGANIZATION

SACLANTCEN
LA SPEZIA, ITALY

Published by

STI

SACLANTCEN REPORT SR-82

NORTH ATLANTIC TREATY ORGANIZATION

SACLANT ASW Research Centre
Viale San Bartolomeo 400,
I-19026 San Bartolomeo (SP), Italy.

tel: national 0187 540111
international + 39 187 540111

telex: 271148 SACENT I

THE THEORETICAL RESPONSE OF A VERTICAL LINE ARRAY TO WIND-GENERATED NOISE IN SHALLOW WATER

by

Rachel M. Hamson

15 December 1984

This report has been prepared as part of Project 21.

APPROVED FOR DISTRIBUTION

RALPH R. GOODMAN

A-1

TABLE OF CONTENTS

List of Figures

Table of Contents (Cont'd)

List of Figures (Cont'd)

THE THEORETICAL RESPONSE OF A VERTICAL LINE ARRAY TO WIND-GENERATED NOISE IN SHALLOW WATER

by

Rachel M. Hamson

ABSTRACT

A wave-theory model for the propagation of noise from a surface source layer has been used to investigate the directional response of a vertical array of hydrophones to wind noise in shallow water. The model assumes an infinite layer of sources radiating sound with pressure directionality of the form $\cos^m\alpha$, where $m > 1$ and α is an angle measured from the downward vertical. The field incident on the array is inhomogeneous and directional responses have been calculated from the (non-Toeplitz) spatial correlation matrix for various bottom types, sound speed profiles, and values of m up to 3. Results show that both components of the noise field — the discrete normal modes and the continuous spectrum — can contribute significantly to the total noise level and to the array response. Shallow-water noise levels are found to exceed those for an idealized, infinitely-deep ocean by approximately the amount contributed by the discrete modes. Furthermore, the discrete mode arrivals give high-array responses in near-horizontal steered directions. Thus the directional response pattern produced can be of considerably different form from that predicted by a simple correlation model for ideal conditions. The extent of these differences in both noise level and array response is strongly dependent on bottom type and on the value of the parameter m, and slightly dependent on sound-speed profile. Finally, calculations of array response using an approximated Toeplitz matrix, instead of the full correlation matrix, result in large errors under certain conditions, and demonstrate that a one-dimensional vertical correlation function is not a sufficient descriptor of noise in shallow water.

INTRODUCTION

Noise generated by the action of wind at the ocean surface can often be the dominant component of the total underwater ambient-noise field at frequencies above 200 to 300 Hz or in high sea states. Other noise sources, which include local and distant shipping, biologics, seismic activity, etc., make their main contributions in different frequency ranges or at specific locations. It is also commonly accepted <1>, that noise levels at shallow-water sites are higher than those observed in deep ocean environments for the same frequency and wind speed. Wenz <1> found an average difference of 5 dB between collections of noise data from shallow and deep water areas. This increase is supported by measurements carried out by Piggott <2> at a hard-bottom, shallow-water site of 60 m depth. He found noise levels, which were highly correlated with wind speed, that were even higher than those analyzed by Wenz over a frequency range of 100 to 3000 Hz. Wenz also suggested a strong seasonal dependence of the noise, up to 10 dB higher levels in winter than in summer conditions, whereas Piggott's data showed a difference of about 3.5 dB between the two seasons. Those studies referred to omnidirectional noise levels, as measured by single hydrophones, but it seems probable that wind-noise directionality, particularly in the vertical plane, may also be of a different form in shallow water and be dependent on the prevailing environmental conditions.

This report presents a theoretical study of the directional response of a vertical array of hydrophones to wind noise in various shallow-water environments. Three main issues are addressed: (1) the dependence of the noise levels and array response on the bottom type and sound-speed profile, (2) the sensitivity of the results to the assumptions made on the distribution of wind-noise sources, and (3) the effect of array response on the inhomogeneity of the incident noise field caused by shallow-water propagation.

Some comments are in order at this point on the particular problems associated with array-response calculations in a shallow-water situation. The response of a steered array of hydrophones to any general incident acoustic field can be calculated if the complex pressure at each hydrophone position or the complex spatial correlation coefficient between every pair of hydrophones are known. In an ideal environment, with straight line propagation from noise source to hydrophone without interactions with the ocean boundaries, the acoustic field can be reasonably represented by combinations of plane waves arriving at the receivers from specific directions. In such a case the incident field is homogeneous and correlation coefficients depend only on hydrophone separations and not on their absolute positions in the medium.

In shallow water the propagation from either a distant point source, or from a closer distribution of sources that might represent wind noise generation, gives rise to complicated incident fields due to the proximity of both surface and bottom. The field is characterized by the existence of normal modes of propagation and is generally inhomogeneous in the vertical plane. Thus the field cannot be expressed as a sum of plane waves, which

makes the concept of vertical field directionality of either signal or noise rather more complicated than in an infinitely deep ocean. Indeed the field directionality can be investigated only by 'observing it' through the response of a vertical array, which itself is dependent on the particular environment, i.e. the bottom type, sound-speed profile, and the position of the array in the water column.

A brief survey follows of previously published work on various aspects of wind-induced noise.

Theoretical studies on surface-noise generation and propagation can be found in the following papers: Cron and Sherman <3>, Liggett and Jacobson <4>, Linette and Thompson <5>, Talham <6>, Stockhausen <7> and, more recently, Kuperman and Ingenito <8>. These studies all postulate the generation of noise by an infinite sheet of sources at or near the ocean surface, having either a specified source-element directionality <3, 5, 6, 7> or a specified correlation function between horizontally spaced elements <4, 8>. Liggett and Jacobson <4> compare these two approaches and derive source correlation functions that can be identified (for an ideal semi-infinite medium) with pressure radiation directionalities of the form $\cos^m\alpha$, where the source-directionality parameter $m \geq 1$ and the angle α is measured from the downward vertical.

This view of noise generation by an infinite source layer is used in the absence of any established physical theory of surface-wave noise generation at frequencies above about 50 Hz, where the dominant mechanism for inducing acoustic transmission below the surface changes from gravity-wave effects to the impact of spray and whitecaps. (Papers by Franz <9> and Wilson <10> begin to investigate this subject, and other work is also in progress, e.g. Kerman <11>).

Attempts have been made to infer the value of the source-directionality parameter m by comparison with measured data. According to Urick <12>, values of m between 1 and 3 have been suggested, although it is not clear in some of the references quoted by Urick whether m refers to directionality of amplitude or power. Linette and Thompson <5> compared vertical correlation data with modelled results, assuming straight-line propagation, and for frequencies of 700 Hz and 1000 Hz obtained values of $m = 1/2$ for low-wind speeds and $m = 3/2$ for 10 to 15 kn winds. Stockhausen <7> compared his results, which include the effects of bottom reflections, with data from Arase and Arase <13> and Axelrod et al <14> and concluded tentatively that sources radiating power with $\cos^2\alpha$ directionality (i.e. our $m = 1$) adequately describe these data, although he indicated a possible increase of m with sea state and frequency. He also pointed out that the use of more realistic environmental conditions with a particular value of m accounts for as much variation in field directionality as does the change of m in a simple environment. This effect is also found in the vertical array responses of the present study. Since the value of m and its frequency/sea-state dependence is by no means finally established, m is treated as a variable here and results are presented for values of m up to 3.

The theoretical studies listed above treat the environment in various ways. Cron and Sherman <3> assume straight-line ray propagation in a semi-

infinite medium and derive the spatial correlation function, for different values of m, between arbitrarily separated receivers well below the ocean surface. Liggett and Jacobsen <4> use a wave-theory approach,also in an ideal medium. Talham <6>, and later Stockhausen <7>, calculate vertical field directionality and include the effects of bottom loss and of variations in sound speed with depth. Stockhausen converts field directionality to complex correlation coefficients by numerical methods. These models all result in plane-wave incidence at a receiver.

Kuperman and Ingenito <8> differ from these approaches by deriving from wave theory the spatial correlation function for a stratified ocean and representing the propagation from every point of the source layer by the full solution of the wave equation. This includes the discrete normal modes and the continuous modal spectrum (or 'near-field' of the source layer). The latter component is closely related to the field in an idealized, infinitely deep water situation in which no discrete modes exist and the continuous field is the sole contributor to the noise. The sum of the two components for the shallow-water situation is required and a vertically inhomogeneous field is obtained, i.e. the correlation coefficient between two points depends on their depths as well as on their separation (thus the correlation matrix for a vertical array is not of Toeplitz form). The Kuperman-Ingenito model <8> is therefore the most suitable for shallow-water studies and indeed is the only one applicable to the investigation of vertical arrays. An arbitrary source-correlation function is used in the initial formulation, but is later specialized to the case of uncorrelated sources, which can be related <4> to a source pressure directionality of $\cos\alpha$, i.e. $m = 1$. Recent extensions to the model have been made to include more general source correlation functions identifiable with $\cos^m\alpha$ directionalities, where $m > 1$.

This extended version of the Kuperman-Ingenito model forms the basis of the present study, and is used to determine the effects of environmental parameters and source directionality on both noise levels and array response pattern.

Absolute noise levels can be obtained from such a model by scaling the results by a source-level factor, q, which is a function of wind speed and frequency. Recent work on wind-noise source-levels include an empirical model by Wilson <10> for wind speeds between 10 and 50 kn and frequencies from 50 Hz to 1000 Hz, and a study using the current model by Wolf and Ingenito <15>. The latter study used the model to remove site dependence (propagation effects) from measured noise levels taken at five different sites for wind speeds up to 25 kn and two chosen frequencies, 500 Hz and 1000 Hz. It produced estimates of q that differed considerably from Wilson's results. Ferla and Kuperman <16> also use this model to analyze data from one particular soft-bottom site and derive source levels from measured noise levels for a frequency range of 400 to 3200 Hz and wind speeds of 10 to 40 kn. Their results compare well with those of Wilson over the limited frequency range in which comparison is possible. All these source level studies assume a $\cos\alpha$ source-pressure directionality.

The present study computes results for a unit source level, since this allows the influence of various parameters to be investigated. Absolute

noise levels and array power output can be found by applying a scaling factor, q, that is appropriate to the wind/frequency conditions.

The report is organized as follows. Chapter 1 describes the shallow-water model and its extensions in more detail, and states the environmental conditions that will be used. These include three sets of bottom conditions that correspond to real areas and are representative of a soft bottom, a very hard bottom, and an intermediate bottom. Sound-speed profiles for winter and summer are used, as well as a theoretical isovelocity case. Thus the results cover a range of realistic conditions likely to be encountered at sea.

The results for calculated noise levels and the directional response of a vertical array are presented in Chap. 2. Generally an array of 11 hydrophones centred at mid-depth in 100 m of water is considered, with hydrophone spacings close to half-wavelength ($\lambda/2$) at two frequencies, 150 Hz and 480 Hz; a few examples of a 21-element $\lambda/2$ array are also included. Section 2.1 tabulates noise levels at mid-water depth as functions of bottom type and frequency for the souce-directionality parameter $m = 1$ and 2. Comparison is made with the idealized 'deep' water levels from the Cron and Sherman model <3>. Section 2.2 presents the directional response of a vertical array in the various environmental conditions for the discrete-mode and continuous-spectrum components of the noise field separately, and for the combination. These are also compared with results for an ideal medium obtained from the Cron and Sherman model. Section 2.3 investigates the effects of varying the source-directionality parameter, m, between 1 and 3. Section 2.4 compares the exact array response calculations with results obtained if the correlation matrix from the shallow-water model is approximated to a Toeplitz form, i.e. the field is assumed to be homogeneous. Conditions under which this approximation produces unacceptable errors are given.

1 THE SHALLOW-WATER NOISE MODEL

1.1 Model Description

The mathematical derivation of the spatial correlation function of surface-generated noise in a stratified ocean is given in <8>. The situation is summarized in Fig. 1. An infinite layer of monopole sources is located just below the ocean surface, the sources having specified levels and correlations. It has been shown <4> that this is equivalent to modelling a layer of statistically independent directional sources coinciding with the ocean surface when the source correlations and the source directionalities have particular relationships. That is, for sources having pressure radiation directionalities of the form $\cos^m\alpha$, where the angle α is measured from the downward vertical and where the parameter m is a positive integer, the equivalent source corrrelation functions, N, can be expressed as

$$N(\rho) = 2^m m!\, Jm(k\rho)/(k\rho)^m, \qquad m > 1$$

$$= 2\delta(\rho)/(k^2\rho), \qquad m = 1 \qquad \text{(Eq. 1)}$$

where ρ = distance between source elements,
k = wave number.

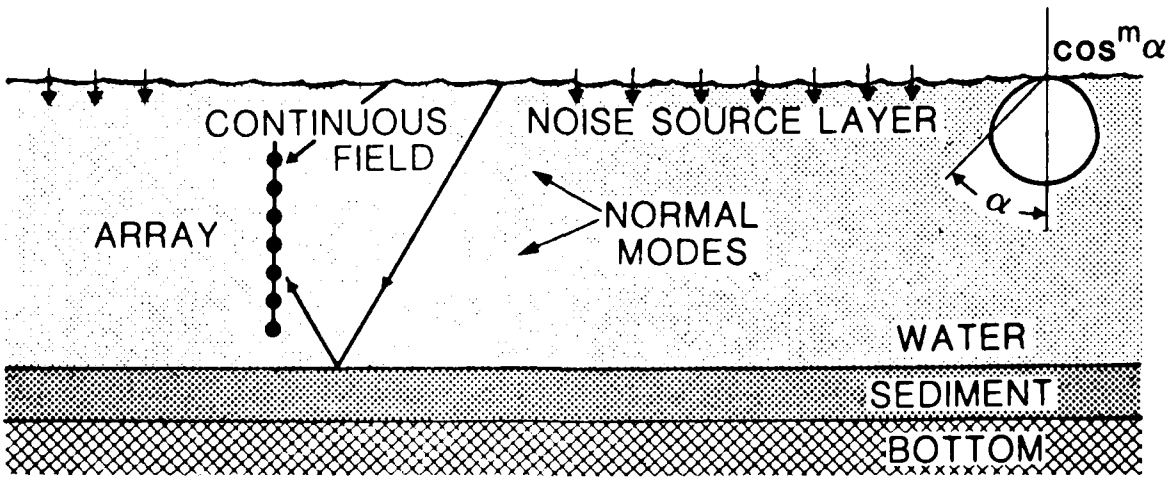

FIG. 1 THE SHALLOW WATER MODEL ENVIRONMENT.

The noise field generated in the water column is determined by the solution of the wave equation for specified environmental conditions. The full solution for a single source is composed of a) a set of discrete normal modes that arise from interactions with the sea bottom at grazing angles less than the critical angle, and b) the continuous modal spectrum caused by direct paths and bottom interactions at steeper angles than critical (Fig. 1). This continuous field is rapidly attenuated with increasing range, and is usually neglected in studies of propagation from distant sources. However, it is essential to include this component here, since the noise sources on the surface directly above the array can be important contributors. Indeed, in an infinitely deep environment it is this component that provides the total noise, since no discrete normal modes exist.

The spatial correlation function, C, of the noise between any two points is formed from these solutions together with the source correlation function by integration over the infinite surface of sources, as given by the following equation, (Eq. 12 of <8>):

$$C(R,z_1,z_2) = 2\pi q^2 \int N(\bar{\rho})\,d\bar{\rho} \int_0^\infty J_0(n\,|\,\bar{R}-\bar{\rho}\,|)\,g(n,z_1,z')g^*(n,z_2,z')n\,dn\,, \quad \text{(Eq. 2)}$$

where

q = source-level factor
R = horizontal distance between the two points
z_1, z_2 = depths of the two points
z' = depth of the source layer
J_0 = zeroth order Bessel function

and

g is related to the Greens function (see <8>) and satisfies the equation:

$$\frac{d^2g}{dz^2} + \left[k^2(z)-n^2\right]g = -\frac{1}{2\pi}\,\delta(z-z') \quad . \qquad \text{(Eq. 3)}$$

In <8> the m=1 expression for $N(\rho)$ from Eq. 1 is used in Eq. 2 for C. For the general form of $N(\rho)$ some further derivation is required. This is given in App. A of the present report, the resulting correlation function being

$$C(R,z_1,z_2) = \frac{8\pi}{k^{2m}}\,q^2\,m \int_0^k J_0(nR)g(n,z_1,z')g^*(n,z_2,z')(k^2-n^2)^{m-1}\,n\,dn\,. \quad \text{(Eq. 4)}$$

C can be decomposed into two parts, that due to the continuous field and that due to the discrete-mode field. For the discrete-mode contribution, Kuperman and Ingenito <8> continue the derivation and obtain an expression

Figure 8 gives examples of results for the source-directionality parameter m = 1, 2 and 3 plotted together. The three plots are for the 5λ (11-element) array at 480 Hz in isovelocity/hard-bottom conditions and show the total response and the response to the separate components, discrete modes and continuous field. These results are all normalized with respect to the average hydrophone level of the total field for the m = 1 case (=11.3 dB). Thus the figure shows not only the differences in response pattern but also the decrease in noise level as m increases and as more energy is lost by the high bottom interaction of the high-order modes. The response to both field components decreases as m increases, particularly in directions towards the horizontal. The discrete-mode response suffers very high attenuation, the omnidirectional level being reduced by over 15 dB between m = 1 and m = 3, and the relative importance of the continuous component increases. However, the mode arrivals are still evident as maxima either side of broadside on the m = 3 total-response plot for this hard-bottom case.

Figure 9 shows results in identical conditions, but with the soft bottom. The total responses for the source-directionality parameter m = 1, 2 and 3 are given on the left-hand plot, normalized to the m = 1 omnidirectional level of 7.3 dB. In this case the total noise is decreased by 7.1 dB between m = 1 and m = 3, and again the near-horizontal response of the array to the discrete modes is much reduced. The right-hand plot, which is normalized to the m = 3 omnidirectional level of 0.2 dB, shows the separate components for the m = 3 case. Here the discrete-mode contribution has become so attenuated that it is negligible compared with the continuous component.

The results of Figs. 8 and 9 indicate that change of the source directionality between $\cos\alpha$ (i.e., m = 1) and $\cos^3\alpha$ (i.e., m = 3) has a considerable effect on both the omnidirectional level and the directional pattern of the array response, more so than that caused by the change of sound-speed profile discussed in Sect. 2.2.

2.4 Comparison of exact Array Response with those obtained using an approximated Toeplitz correlation matrix

As demonstrated mathematically in <8>, the noise field in a stratified ocean is inhomogenous in the vertical plane. Here we consider the extent of this inhomogeneity and hence the degree to which the spatial correlation matrix for a vertical array is of non-Toeplitz form. Examination of the matrices output by the noise model for the two separate components of the field (discrete modes and continuous spectrum) has shown the continuous-spectrum field to be more homogenous than the discrete-mode field, and the imaginary parts of both to be more homogenous than their respective real parts. However, the clearest way to show the effects on array response is to carry out the calculation under the assumption of a homogenous field and to compare the result with the exact calculation.

To do this, the (N-1) complex coefficients that make up the first row of the matrix $[C_{np}]$ were used to create a Toeplitz matrix on the assumption that correlation coefficients between pairs of hydrophones having the same spacings are equal. This new matrix is composed of correlation coefficients referred to the shallow end of the array. Since the field is not truly homogeneous, a different Toeplitz matrix and different errors in array response are obtained if coefficients are referred to the other end

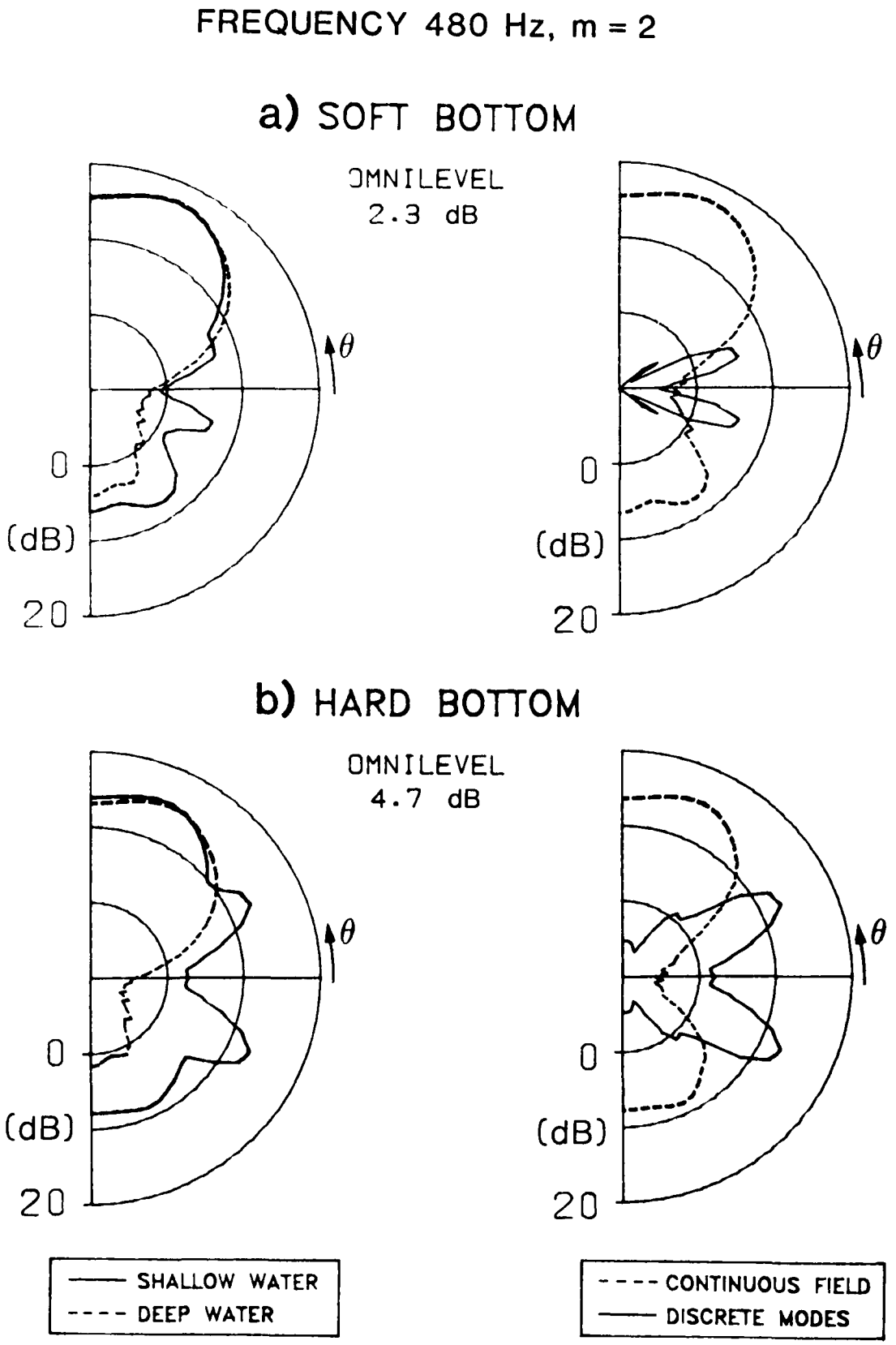

FIG. 7 VERTICAL ARRAY RESPONSES AT 480 Hz FOR AN ISOVELOCITY SOUND-SPEED PROFILE AND SOURCE-DIRECTIONALITY PARAMETER m = 2. a) SOFT BOTTOM CONDITIONS b) HARD BOTTOM CONDITIONS

Array response results for the winter and summer sound-speed profiles are plotted in Fig. 6a for the 5λ (11-element) array at 150 Hz. These are for the soft bottom and the source-directionality parameter m = 1. The summer case (dotted curve) shows a 6 dB null around broadside, which does not occur in the winter case; otherwise there is little difference between them. The change of profile has the effect of changing the shape of the discrete modes, particularly in the first 50 m of water where the two profiles differ most. Thus sources just below the surface excite the modes to different extents in the two environments. In the summer case, higher order modes, representing steeper incidence at the hydrophones and having greater losses in the bottom, are excited more than the lower order modes, which 'arrive' close to broadside. In the winter case these lower order modes are also present. The omnidirectional level in winter is 1.2 dB higher than in summer.

Figure 6b shows the results for the 5λ (11-element) and the 10λ (21-element) arrays for the summer case, plotted together. The longer array almost spans the water column and hence covers most of the changing sound speed of the summer profile. However, there is little difference between the two patterns, apart from an almost constant 3 dB increase in array power for the 10λ array due to the higher gain. Thus the results of Fig. 6 indicate that change of sound-speed profile does not have such a large effect on array response or omnidirectional level as do the changes in bottom type that were compared in Figs. 3 to 5.

2.3 The Effect of Source Directionality on Directional Array Response

The results obtained with the source-directionality parameter m = 2 for the 5λ (11-element) array at 480 Hz are given in Fig. 7. This figure is directly comparable to Fig 3, which shows results for m = 1 , and contains plots for the a) soft and b) hard bottom types for an isovelocity profile. The Cron and Sherman 'deep-water' result <3> (dotted curves on the left-hand plots) has an omnidirectional level of 2 dB for m = 2. For the soft bottom the broadside shallow-water response is very close to the 'deep-water' level; whereas for the hard bottom it is 7 dB above the 'deep-water' response. The shallow-water omnidirectional levels are much lower than the m = 1 case of Fig. 3; by 5 dB for the soft bottom and 6.6 dB for the hard bottom. This is mainly due to higher losses of the discrete modes as m increases. Equation 5 indicates how the higher order modes (having smaller wave number K_n and hence larger factor $(k^2-K_n^2)^{m-1}$) are weighted more than the lower order modes, which have steeper arrival angles at a receiver and suffer considerable bottom loss. This effect is illustrated in Fig. 7b by a deeper null (of up to 10 dB) at broadside than in the m = 1 case, and by narrower maxima in the arrival directions of high-order modes. Overall, for m = 2, the discrete-mode component is reduced and the continuous field becomes (relatively) more important. This is particularly evident for the soft bottom, where, apart from the lobe below broadside, the total response is fairly well represented by the continuous component alone. Again, this latter component is close to the Cron and Sherman response pattern, except for the vertically downward directions (45° to 90°) where bottom returns are seen in the shallow-water case.

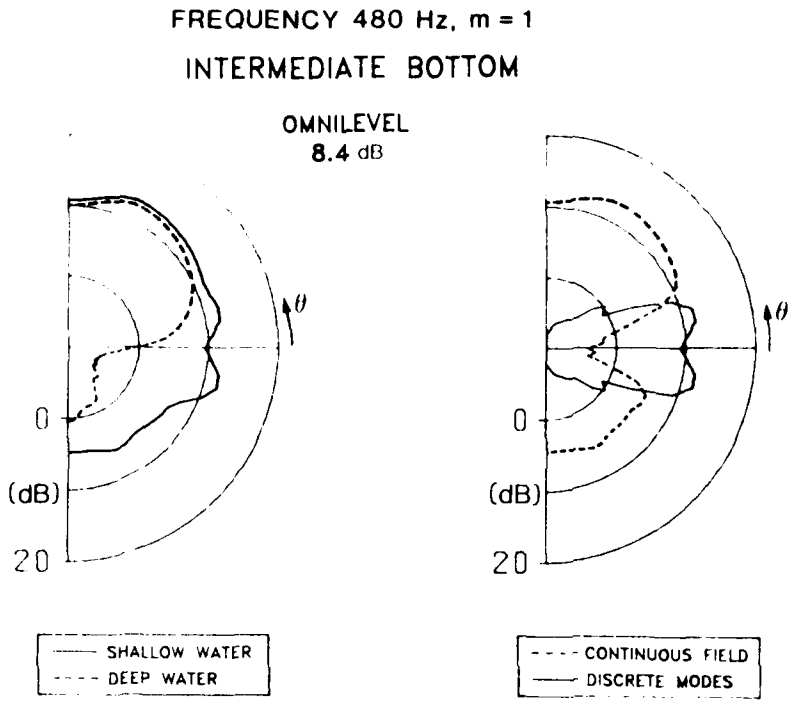

FIG. 5 VERTICAL ARRAY RESPONSES AT 480 Hz FOR AN ISOVELOCITY SOUND-SPEED PROFILE AND SOURCE-DIRECTIONALITY PARAMETER m = 1, FOR THE INTERMEDIATE BOTTOM TYPE.

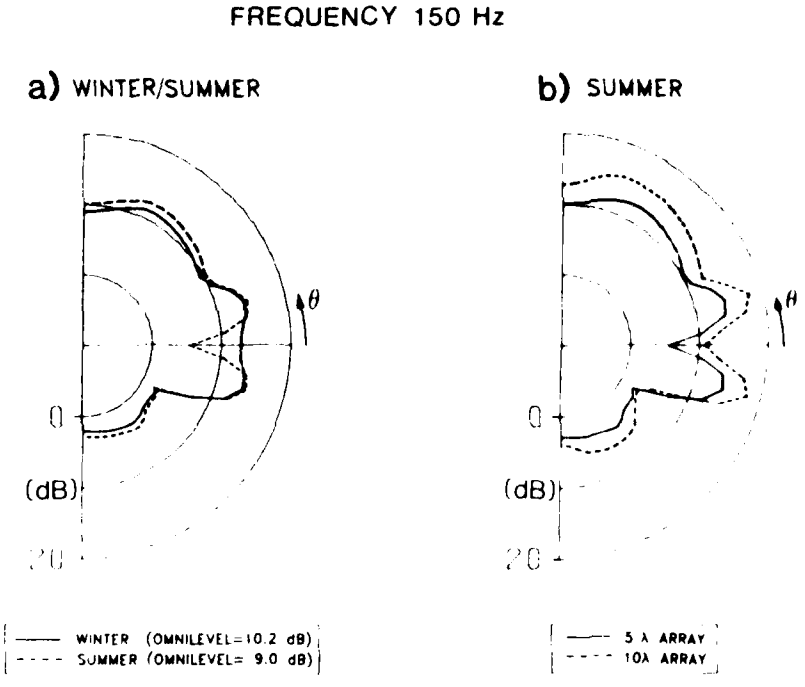

FIG. 6 VERTICAL ARRAY RESPONSES AT 150 Hz FOR SOFT BOTTOM CONDITIONS, AND THE SOURCE-DIRECTIONALITY PARAMETER m = 1.
a) Winter and summer compared, 5λ array.
b) 5λ and 10λ arrays compared in summer.

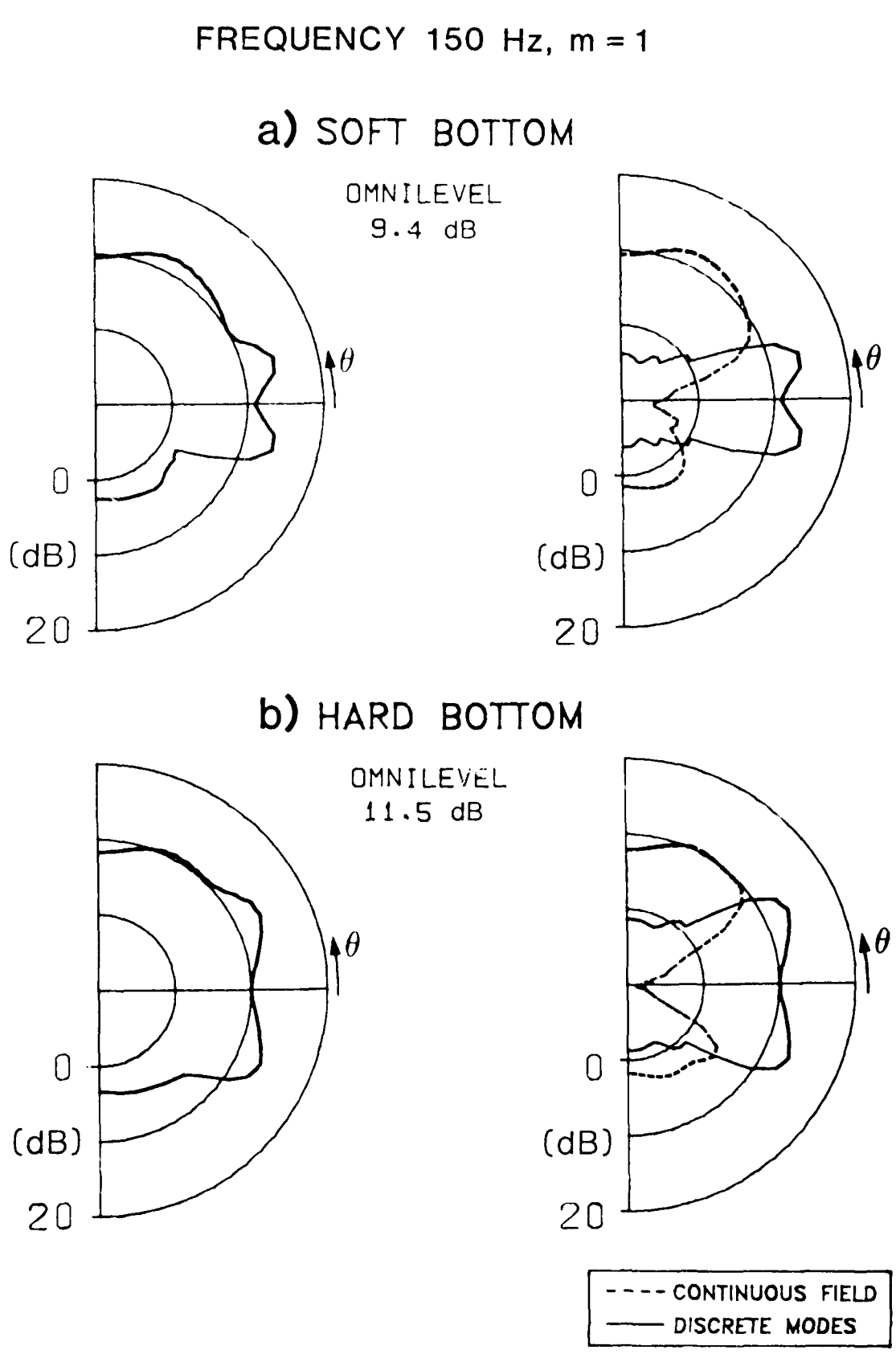

FIG. 4 VERTICAL ARRAY RESPONSES AT 150 Hz FOR AN ISOVELOCITY SOUND-SPEED PROFILE AND SOURCE-DIRECTIONALITY PARAMETER m = 1. a) SOFT BOTTOM CONDITIONS b) HARD BOTTOM CONDITIONS

The hard-bottom results of Fig. 3b show an even greater departure from the 'deep-water' result. The omnidirectional level is increased to 11.3 dB, which is 6 dB above the Cron and Sherman level, and the array response has almost as much power from the bottom as from the surface; the maximum power, though, is at about ± 25° from broadside due to the discrete-mode arrivals. The higher critical angle for this bottom (35°) provides a wider angular sector about broadside containing discrete modes. At broadside itself the response is increased by 11 dB over the 'deep-water' response. It is seen again that the result for the continuous field in the shallow water is similar to the Cron and Sherman 'deep-water' result above broadside; below broadside it shows a higher level than either the Cron and Sherman result or the soft-bottom result. This is due to the highly reflecting bottom. However, the results for both bottom types show that the primary cause of the increased omnidirectional level and of the very different form of the array-response pattern from that in the 'deep-water' case is the discrete-mode component of the field. It is this component that is very sensitive to the particular bottom type.

Figure 4 shows the results obtained with a) soft and b) hard bottom types by reducing the frequency to 150 Hz. The format of the figure is the same as Fig. 3, and the results are for the source-directionality parameter m = 1 and an isovelocity profile. At this frequency, and with a near-$\lambda/2$ spacing, the 5 λ (11-element) array spans a larger portion of the water column (about half) than at 480 Hz. The Cron and Sherman 'deep-water' result, being dependent only on hydrophone spacing in wavelengths, would be the same as that shown in Fig. 3, and is omitted in this figure. The soft-bottom result at 150 Hz has an omnidirectional level that is 2 dB higher than at 480 Hz. This is due to reduced attenuation of the discrete modes. It is seen in Fig. 4 that the response to this component on either side of broadside protrudes from the rest of the pattern rather more than in Fig. 3. Thus the transition between the contributions of the two components at the critical angle of 20° is even more pronounced at 150 Hz. For the hard bottom the results are very similar to the 480 Hz results, the omnidirectional level being within 0.2 dB. This is due, as mentioned in Sect. 2.1, to the compensating effects of the way in which shear losses and compressional-wave attenuation change between these two frequencies.

Figure 5 completes the results for the three bottom types for isovelocity/m=1 conditions, by presenting the array responses for the intermediate bottom at 480 Hz. The left-hand plot gives the total response in shallow water and the Cron and Sherman 'deep-water' result (dotted curve). The right-hand plot shows the two separate components of the shallow water result. Comparison with Fig. 3 for the other two bottom types at the same frequency shows that the general shape of the array response is closer to that of the soft bottom. This is because these two bottom types have almost equal critical angles, and that these control the size of the angular sectors in which the separate components (of the right-hand plot) make their main contributions. The continuous component in this intermediate-bottom case shows higher levels below the horizontal (by up to 3 dB) than for the soft bottom, due the absence of an absorbent sediment layer. The omnidirectional level of 8.4 dB lies between the soft and hard bottom omnidirectional levels for this frequency, and thus the departure of the shallow-water result from the Cron and Sherman 'deep-water' result is also intermediate between these two cases.

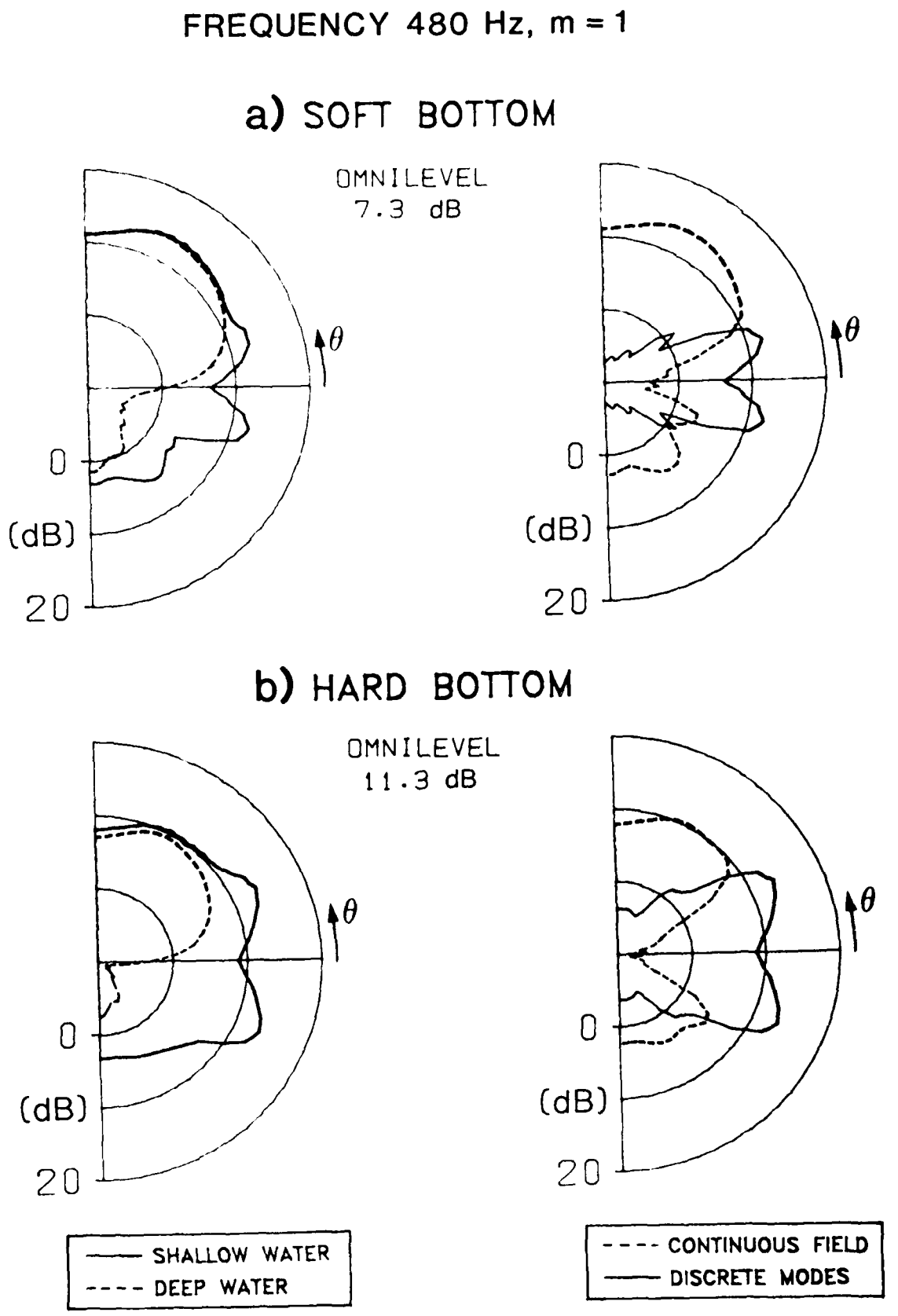

FIG. 3 RESPONSES OF A 5λ VERTICAL ARRAY AT 480 Hz FOR AN ISOVELOCITY SOUND-SPEED PROFILE AND SOURCE-DIRECTIONALITY PARAMETER m = 1. a) SOFT BOTTOM CONDITIONS b) HARD BOTTOM CONDITIONS

(11-element) arrays are therefore 45 m and 14.7 m respectively; hence the 10 λ (21-element) array at 150 Hz almost fills the 100 m water column.

Directional responses have been calculated as the array is steered vertically in 5° steps from endfire looking vertically up to the surface, through broadside, to endfire looking vertically down to the bottom. The results are presented in Figs. 3 to 6 as polar plots of $P(\theta)$ in decibels, normalized to the average power of the 11 (or 21) hydrophones, for a unit source level. The average hydrophone power (or omnidirectional level) is written next to each plot. Thus these results can be viewed as array noise gain. The absolute beam levels can be obtained from the plots by the decibel addition of the omnidirectional level and a suitable source level. This normalization convention is followed throughout the report unless otherwise stated.

The shallow-water results are compared with array responses calculated from the Cron and Sherman model so as to give a representation of the situation in an ideal, infinitely deep ocean. The equations for the Cron and Sherman correlation function between vertically spaced receivers are reproduced in App. D.

Figure 3 shows the 480 Hz results for the 5 λ (11-element) array for a) soft and b) hard bottom types for the source-directionality parameter m = 1. These are for an isovelocity sound-speed profile. The plots on the left show the array response to the total shallow-water field (solid curves), with the Cron and Sherman 'deep-water' result superimposed (dotted curves). The plots on the right show the decomposition of the shallow water results into their two components: the continuous-spectrum and discrete-mode responses (the total response is the power sum of these two components). The Cron and Sherman result, which is independent of the environment, appears smaller in the lower plot than in the upper plot because the results are normalized with respect to omnidirectional levels of 11.3 dB and 7.3 dB respectively.

Inspection of Fig. 3 shows that the responses for shallow water differ significantly from the ideal 'deep-water' result. The extent of this difference is strongly dependent on bottom hardness. The 'deep-water' result (which has an omnidirectional level of 5 dB) shows all the power arriving from above the horizontal, and particularly from near-vertical directions. This is a consequence of the Cron and Sherman assumptions. (The low-level response in the vertically downward direction is due to array sidelobes and the beginning of a grating lobe). The soft-bottom shallow-water result, with an omnidirectional level of 7.3 dB, shows arrivals clearly from near-horizontal and vertically downward directions. The response at broadside is 6 dB above the deep-water level. It is seen from the plot of the response to the two separate components that the discrete modes provide the high responses either side of broadside and that the continuous field provides the arrivals from nearer to the vertical. Thus the two components are dominant in their own particular angular sectors, the boundary between them being the critical angle for this bottom type (20°). Note that the Cron and Sherman result on the left of Fig. 3a is very similar to the continuous response above the horizontal in the right-hand plot. Below the horizontal they differ considerably, as the continuous field in shallow water contains bottom-reflected energy.

It should be noted that there are other loss mechanisms, due to surface and bottom roughness, that have not been included in this study. These could have a considerable effect (in high sea-states for example) on high-frequency discrete-mode fields, and could therefore change the relative contributions of the two components of the total field.

Table 3 gives noise levels when the source-directionality parameter m = 2; the continuous components are now comparable with the 1.96 dB (10 log $\pi/2$) Cron and Sherman level. Again the intermediate bottom gives rise to slightly higher continuous field levels than the other two. The discrete-mode levels are considerably lower for m = 2 than for m = 1 (Table 2) for all bottom types. The total field level is thus dominated by the continuous component, except for the hard bottom where the two contributions remain comparable. It is seen from Eq. 5 for the discrete-mode contribution, that as the value of m increases the higher order modes (which have smaller wave numbers, K_n) receive increasingly more weight than the lower order modes. These higher order modes have steeper 'angles of incidence' and the resulting increased bottom interaction gives rise to greater attenuation.

One can make the general conclusion here that noise levels in shallow water are higher than those in 'deep' water by roughly the amount contributed by the discrete modes. Tables 2 and 3 show that the contribution of this discrete-mode component decreases with increasing frequency, higher source directionalities, and more absorbent bottom conditions. At high enough frequencies the omnidirectional level may be well represented by the continuous field alone. However, as we shall see in the following sections, neither field component can be neglected in calculating the directional response of a vertical array, since both contributions have certain directions in which they are dominant.

Appendix B contains plots of noise level vs depth over the 100 m water column for some selected conditions. These show depth variations of generally less than 2 dB, apart from higher differences near the surface and bottom.

2.2 Environmental Dependence of the Directional Response of a Vertical Array

The power response, $P(\Theta)$ of an array of hydrophones steered to direction Θ, can be calculated from the matrix of complex correlation coefficients between all pairs of hydrophones. The appropriate equations are given in App. C. For a homogeneous noise field, such as that assumed by the Cron and Sherman model <3>, this matrix is of Toeplitz form for any equally spaced line array. This would also be the case for a horizontal array in the field of the shallow-water model, but for a vertical array the field inhomogeneity results in a non-Toeplitz matrix (i.e. a Hermitian matrix comprising N(N-1)/2 unique coefficients for an N-element array).

The results in this and the following sections are mainly for a uniform vertical array of 11 elements, centred at 50 m depth, although a few cases of 21-element arrays are also included. The hydrophones are spaced at just less than $\lambda/2$ for the two frequencies (150 and 480 Hz) under consideration (i.e. spacings of 4.5 m and 1.47 m). The physical lengths of the 5 λ

TABLE 2

NOISE LEVELS AT 50 m DEPTH, dB, RELATIVE TO UNIT SOURCE LEVEL
FOR DIFFERENT BOTTOM TYPES AND AN ISOVELOCITY SOUND-SPEED PROFILE IN 100 m WATER DEPTH
WITH THE SOURCE-DIRECTIONALITY PARAMETER m = 1

Bottom Type	FREQUENCY					
	150 Hz			480 Hz		
	Total field	Continuous field	Discrete-mode field	Total field	Continuous field	Discrete-mode field
Hard (SWAP)	11.6	5.8	10.3	11.3	5.3	10.0
Intermediate (Sicily)	8.6	6.1	5.0	8.4	6.0	4.7
Soft (S.E. Elba)	9.3	5.2	7.2	7.3	5.1	3.4

TABLE 3

NOISE LEVELS AT 50 m DEPTH, dB, RELATIVE TO UNIT SOURCE LEVEL
FOR DIFFERENT BOTTOM TYPES AND AN ISOVELOCITY SOUND-SPEED PROFILE IN 100 m WATER DEPTH
WITH THE SOURCE-DIRECTIONALITY PARAMETER m = 2

Bottom Type	FREQUENCY					
	150 Hz			480 Hz		
	Total field	Continuous field	Discrete-mode field	Total field	Continuous field	Discrete-mode field
Hard (SWAP)	4.6	2.0	1.2	4.7	2.0	1.4
Intermediate (Sicily)	3.0	2.7	-9.0	2.9	2.7	-9.5
Soft (S.E. Elba)	2.8	2.2	-6.3	2.3	2.0	-8.5

2 MODELLED RESULTS FOR NOISE LEVELS AND THE DIRECTIONAL RESPONSE OF A VERTICAL ARRAY

2.1 Omnidirectional Noise Levels

The noise level, NL, due to a source level, SL, for an ideal, infinitely deep ocean can be derived from the Cron and Sherman equations <3>, resulting in the simple relation.

$$NL = \pi/m \; SL,$$

where m is the source-directionality parameter.

This equation is independent of depth and the particular environment. Under such conditions of infinite depth the noise field is represented by the continuous-spectrum component alone, since no discrete modes exist. The factor π/m therefore forms a lower bound for the shallow-water continuous field (in isovelocity conditions), since this contains not only direct paths but also energy from bottom reflections.

Examples of noise levels, relative to unit source level, obtained from the shallow-water model are given in the form of tables of noise levels at 50 m depth vs bottom type, for two frequencies and for the source-directionality parameter $m = 1$ (Table 2) and $m = 2$ (Table 3). These are all for an isovelocity sound-speed profile. The total field intensity is composed of the power sum of the two components: the continuous field and the discrete-mode field. It is seen in Table 2 that the levels of the continuous field are slightly above the 4.97 dB ($= 10 \log \pi$) Cron and Sherman 'deep-water' level, and that the highest level (by 1 dB) corresponds to the intermediate bottom type. The reason for this is that the critical angle for this bottom is smaller than that of the hard bottom, (i.e. a larger portion of the incident noise is included in the discrete-mode component for the hard-bottom case) and the bottom reflectance for the intermediate case is higher than that of the soft bottom.

Table 2, which gives noise levels when the source-directionality parameter $m = 1$, shows that both components of the field make a significant contribution to the noise for all bottom types, although the discrete-modes dominate for the hard bottom. The discrete mode levels for both frequencies vary considerably between the three bottom types, by up to 6.6 dB, whereas the continuous field is less sensitive to this parameter. The total levels differ by up to 4 dB between bottom types. At 150 Hz the noise for the intermediate bottom is 1 dB lower than that for the soft bottom; this is due to shear losses in the intermediate bottom. The situation is reversed at 480 Hz, where shear effects are less; here the soft bottom gives the lowest noise levels, as normally expected. Comparison of the levels for the two frequencies shows a reduction of 2 dB for the soft bottom at 480 Hz, due to the greater attenuation of the discrete modes. The other two bottom types have similar levels at both frequencies, since the higher volume and compressional-wave attenuations at 480 Hz are offset by the reduced effects of shear at this frequency.

Three sound-speed profiles have been used in this study, corresponding to winter, spring/summer, and isovelocity conditions, as plotted in Fig. 2. The summer profile, taken from a measurement in June near Elba, shows a 40 m surface layer of constant speed above a steep thermocline between depths of 40 and 50 m, after which the speed increases slightly with depth. Thus a vertical array centred at 50 m spans both the negative and positive sound-speed gradients.

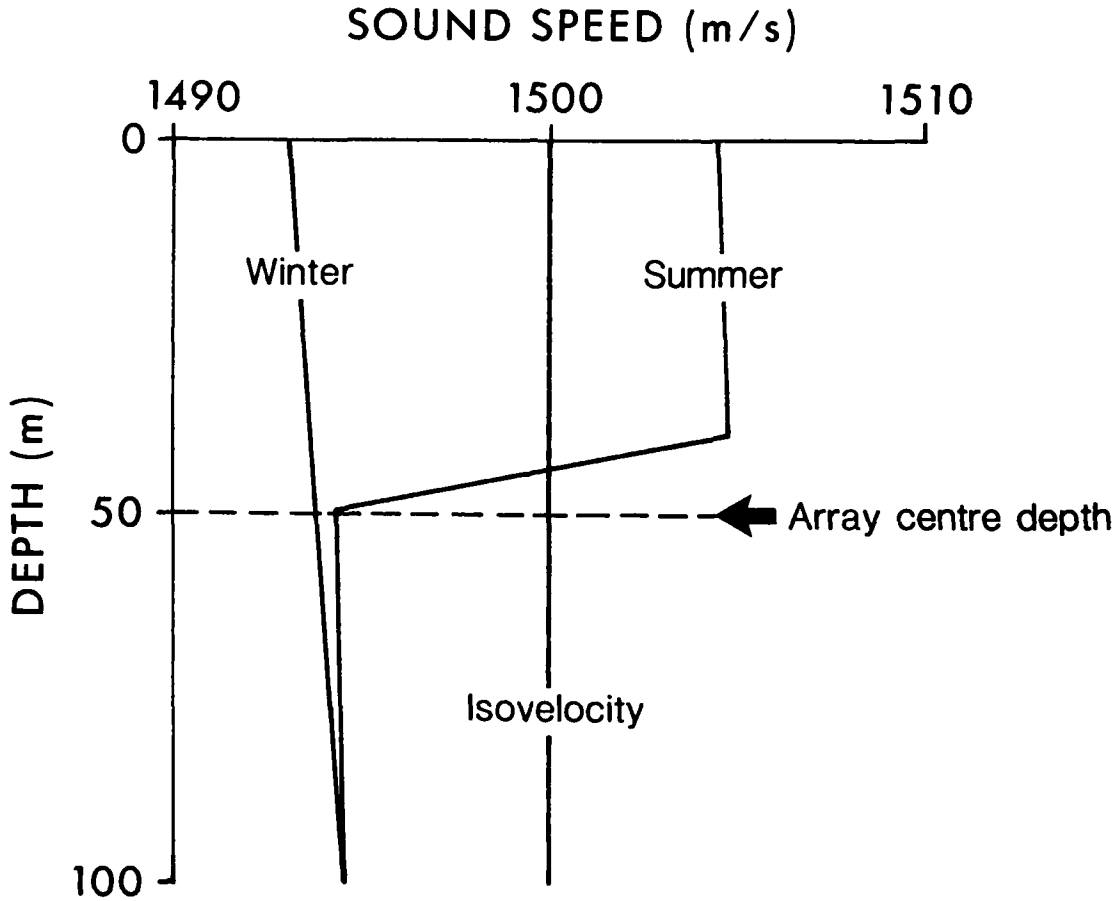

FIG. 2 SOUND-SPEED PROFILES USED IN THE STUDY.

The bottom parameters for three cases are summarized in Table 1. These sets of parameters have been established by detailed modelling studies of propagation-loss data carried out for the three areas, <21, 22, 23> respectively. In all three cases core samples were used to obtain the compressional sound speed and the density, the other parameters being adjusted, within realistic limits, to obtain agreement with the data sets of propagation loss as a function of range and frequency for various source/receiver depth combinations. In the SWAP and Sicily cases it was necessary to include the effects of shear-wave propagation in the sea bed to obtain good comparisons (this is a low-frequency loss mechanism that is not yet fully understood; hence the associated shear speeds and attenuations given should be regarded as tentative). Table 1 shows the SWAP bottom to have the highest compressional speed (1800 m/s), giving rise to the largest critical angle (35°) for acoustic reflections. At the opposite extreme, the Elba bottom case has a low-speed sediment layer above the 1600 m/s bottom, and is the most absorbent of the three types. The Sicily bottom has been denoted 'intermediate' in terms of bottom speed but, as we shall see later, the effect of shear can result in 'lossier' propagation than the Elba conditions at some frequencies.

TABLE 1

BOTTOM PARAMETERS FOR THREE AREAS USED IN THE NOISE MODEL

Area/Type	Relative Density		Compressional Speed m/s		Compressional Attenuation dB/λ		Shear Speed m/s	Shear Attenuation dB/λ
	Sediment	Bottom	Sediment	Bottom	Sediment	Bottom		
SWAP (hard)	-	2.0	-	1800	-	0.8	400	2.0
Sicily (Interme-diate)	-	2.0	-	1610	-	0.75	600	1.5
S.E. Elba (soft)	1.5	1.8	1470-1500 6m sediment thickness	1600	0.06	0.15	-	-

Thus a full description of bottom type requires a knowledge of the many parameters that can influence propagation in different ways. It is not simply a matter of 'hardness', although the terms 'hard' and 'soft' will be used as broad descriptors in this report.

for the correlation function in terms of a summation of mode functions, for the m=1 case. Again for the more general $\cos^m\alpha$ case, the appropriate mathematics are given in App. A, resulting in the following equation for incoherent mode combination

$$C(R,z_1,z_2) \begin{cases} = \frac{\pi q^2 m}{2k^2} \sum_n [u_n(z')]^2 u_n(z_1) u_n(z_2)\, J_0(k_n R) \left(\frac{k^2 - K_n^2}{k^2}\right)^{m-1}, & K_n < k \\ = 0 \quad \text{otherwise} \end{cases} \qquad \text{(Eq. 5)}$$

where K_n = real part of the wave number of the nth mode,
α_n = imaginary part of the wave number of the nth mode,
U_n = the normalized amplitude function of the nth mode.

This reduces to Eq. 30 of <8> if m is set equal to 1. The case of coherent mode summation is discussed in App. A.

A computer model based on the Kuperman-Ingenito theory has been developed at SACLANTCEN by Kuperman and Ferla, for the m = 1 case. The discrete-mode solution (from which the u's, α's and K's are obtained) for specified environmental conditions is provided by the Centre's normal-mode propagation model, SNAP <17>. That model contains a three-layer environment: the water column, the upper layer of the sea bed, and the remaining sea bed extending to infinite depth. The speed of sound can vary with depth in the first two layers. Appropriate densities and attenuation coefficients are input parameters for the two bottom layers. (Range independence of the medium is a basic assumption in the derivation of the noise correlation function <8>).

The continuous field is given by a Fast Field Program (FFP) described in <18, 19>, which is a direct integration of the wave equation over wave number. It is used here for the spectrum of wave numbers up to that of the highest mode. The FFP also takes account of varying sound speed with depth in the water and bottom.

The modifications for the general m case have been inserted into the model. Some sensitivity work has been carried out to establish a value for the depth, z', of the source layer. This should be close enough to the surface such that no further changes in noise level are produced as z approaches the surface. Ingenito <20> suggests that z' should satisfy the condition $z' < \lambda/4$ for wavelength λ. For our two frequencies of 150 Hz and 480 Hz, the depth of the source layer was set to z' = 10 cm.

1.2 Description of Environmental Conditions

This section specifies the particular environmental conditions considered in this report. A water depth of 100 m is used in all cases. Noise levels and the directional responses of a vertical array at the two frequencies have been investigated for three bottom types, corresponding to areas southeast of Elba (soft bottom), in the southwestern approaches to the English Channel (SWAP) (very hard), and in the Strait of Sicily (intermediate).

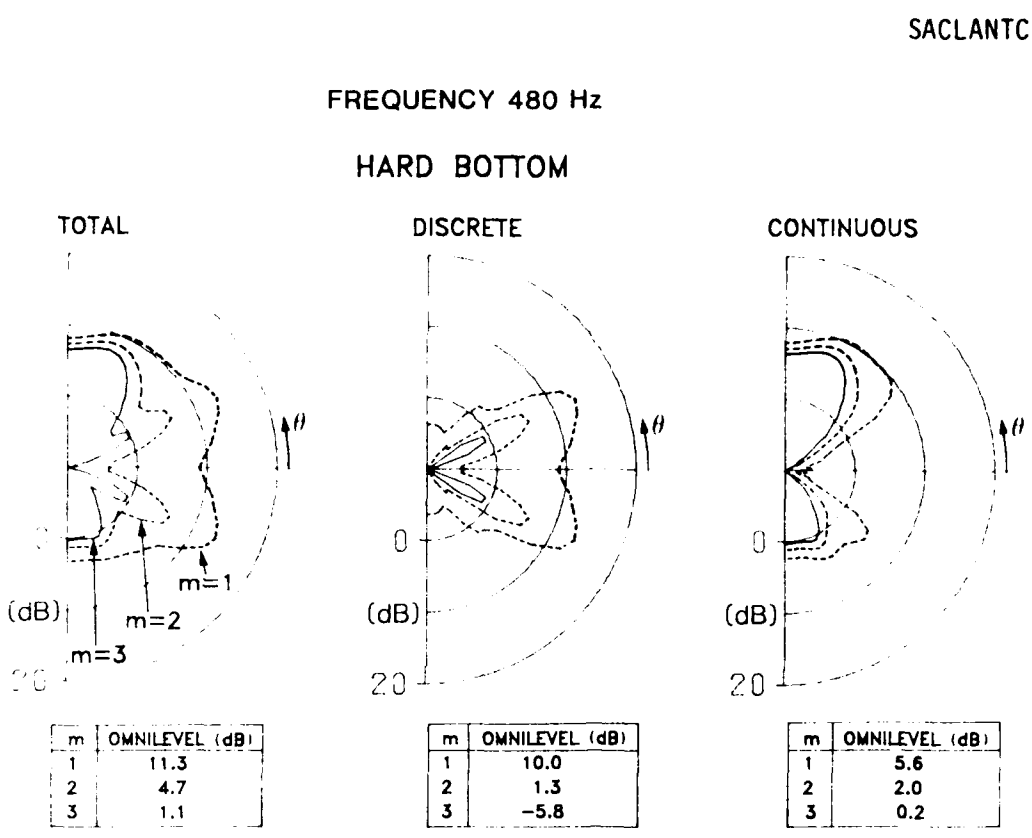

m	OMNILEVEL (dB)
1	11.3
2	4.7
3	1.1

m	OMNILEVEL (dB)
1	10.0
2	1.3
3	−5.8

m	OMNILEVEL (dB)
1	5.6
2	2.0
3	0.2

FIG. 8 VERTICAL ARRAY RESPONSES AT 480 Hz IN ISOVELOCITY/HARD BOTTOM CONDITIONS FOR THE SOURCE-DIRECTIONALITY PARAMETER m = 1, 2 AND 3. Levels are normalized with respect to the average hydrophone power for the m = 1 case.

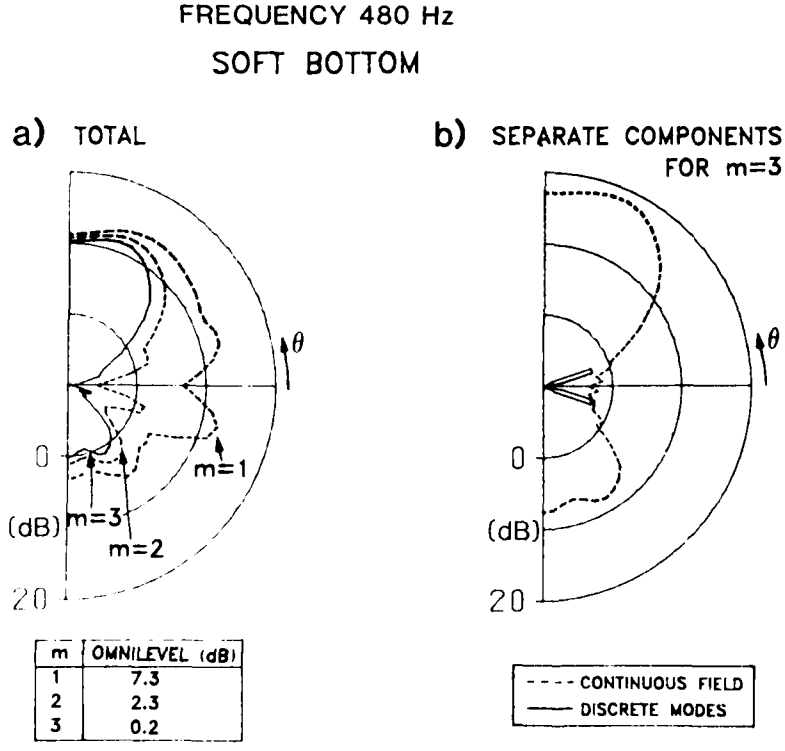

m	OMNILEVEL (dB)
1	7.3
2	2.3
3	0.2

FIG. 9
VERTICAL ARRAY RESPONSES AT 480 Hz IN ISOVELOCITY/SOFT BOTTOM CONDITIONS
a) THE SOURCE-DIRECTIONALITY PARAMETERS m = 1, 2 AND 3,
b) THE SEPARATE COMPONENTS FOR THE m = 3 CASE.

of the array, i.e. using the last column of the original matrix to create a Toeplitz matrix. Some results are given using both Toeplitz matrices.

Figure 10 shows three cases of 5λ (11-element) array responses calculated exactly (solid curves) and calculated using the first Toeplitz matrix (dashed curves). The first two plots are for 150 Hz soft-bottom conditions with either winter or summer sound-speed profiles. In the winter case there is little difference between the two calculations, apart from an error of 5 dB occurring in the downward direction. As expected, there is more discrepancy for the summer conditions, the top half of the array being situated in the thermocline. The largest differences occur at broadside and vertically downward directions. In fact, in the vertically downward directions, for this case, the use of the Toeplitz matrix led to negative power responses (which were set equal to -20 dB for plotting purposes). It has been found that this occurs in many cases, in directions of low noise or directions in which the exact response shows a null. Mathematically, negative power is a consequence of a non-positive-definite correlation matrix; examination of specific Toeplitz matrices that give rise to this effect shows them to contain high, positive or negative, off-diagonal elements, i.e. to be ill-conditioned. It appears that this approximation of an inhomogeneous field in terms of a one-dimensional correlation function introduces some sort of artificiality, and the resulting Toeplitz matrices no longer represent 'real' acoustic fields, since these would always give a positive (or zero) array power response and show side-lobe effects.

The third plot of Fig. 10 gives another example of a prediction by the Toeplitz calculation. The whole sector between 45° below the horizontal and endfire has large errors. This is a 480 Hz case in summer-profile/hard-bottom conditions. Other discrepancies between the Toeplitz and the exact result are a 5 dB difference at broadside and a 2 to 3 dB difference between upward endfire and +45°. However, the response to the dominant mode arrivals at ±30° are reasonably well represented by the Toeplitz method.

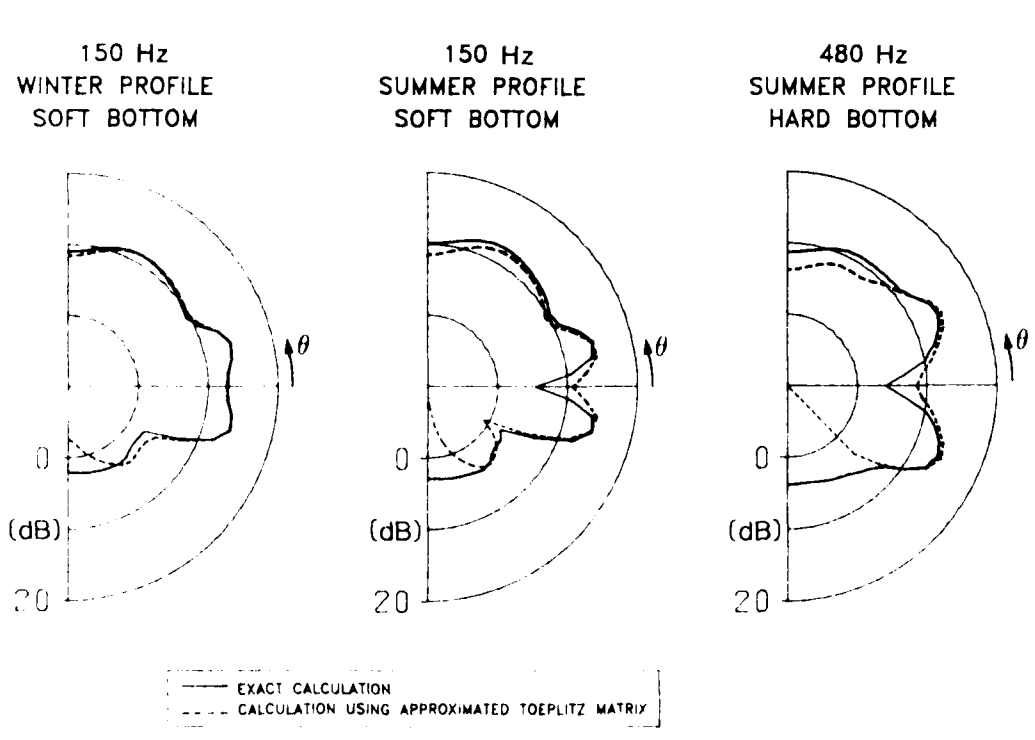

FIG. 10 COMPARISONS OF ARRAY RESPONSES OBTAINED USING THE FULL CORRELATION MATRICES WITH THOSE OBTAINED USING APPROXIMATED 'TOEPLITZ' MATRICES.

A further example is given in Fig. 11 for a 10λ (21-element) array at 150 Hz in summer-profile/hard-bottom conditions. This array spans almost the whole water column. The dashed curves on the two plots were obtained using Toeplitz matrices referred to a) the shallow end and b) the deep end of the array and both show large errors compared with the exact (solid curves) calculation. In Fig. 11a the sector from -45° to endfire is up to 15 dB in error using the Toeplitz method and the broadside response is 5 dB too high. In Fig. 11b the Toeplitz method predicts a minimum at broadside that is 14 dB below the exact result, but in other directions agrees to within 2 to 3 dB.

The examples in this section are for the source-directionality parameter m = 1. For higher values of m, results obtained using the Toeplitz approximation still exhibit errors, but they are generally less evident. As m increases, the contribution of the discrete-mode field is reduced, and the total field becomes more homogeneous (except with extreme sound-speed profiles).

In summary we can state that the Toeplitz approximation gives unacceptable array-response errors in conditions where the discrete-mode field dominates, or where the sound speed varies significantly over the array aperture. These errors occur in low-noise directions, often where the exact response pattern shows a null. The maxima of the response patterns however are usually well estimated by the Toeplitz method.

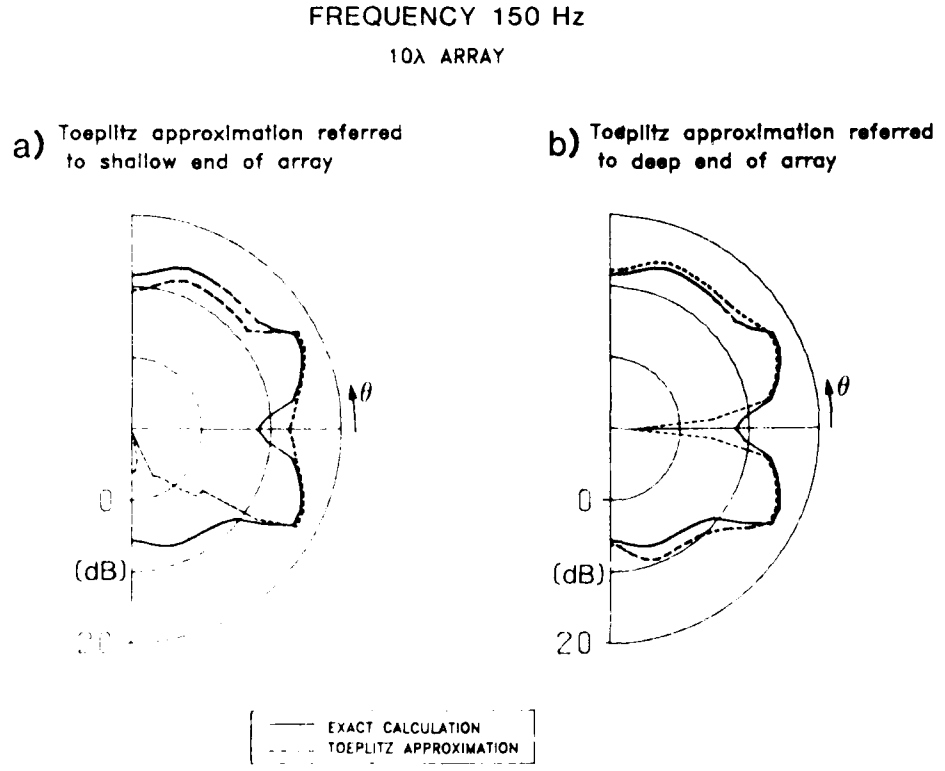

FIG. 11 COMPARISONS OF ARRAY RESPONSES OBTAINED FROM THE EXACT AND APPROXIMATE CALCULATIONS FOR A 10λ ARRAY AT 150 Hz.
a) referred to shallow end of array
b) referred to deep end of array

CONCLUSIONS

The directional response of a vertical array to surface-generated wind noise in shallow water has been calculated under various environmental conditions using the matrix of complex correlation coefficients output by a wave-theory model. The source (pressure) directionalities considered are of the form $\cos^m\alpha$, where the angle α is measured from the downward vertical and the parameter m has values up to 3.

Results show that both omnidirectional levels and array-response patterns can be significantly different from those obtained for a homogeneous semi-infinite ocean ('deep water') using the Cron and Sherman correlation model <3>. Noise levels are higher in shallow water by roughly the amount contributed by the discrete-mode component of the noise field. This quantity is controlled by the environmental parameters, particularly the bottom type, and by the source-directionality parameter m, e.g. for a particular hard-bottom case and for $m = 1$ the noise level in 100 m water depth exceeds the 'deep-water' level by 6 dB at 480 Hz. This increase is of the same order of magnitude as that indicated by measurements reported by Wenz <1> and Piggot <2>. The harder the bottom, the more the discrete modes dominate the other component of the total noise field — the continuous spectrum. This latter component would be the sole contributor in infinitely deep water; in shallow water it is slightly dependent on the environment, but is generally only 1 to 2 dB above the 'deep-water' level.

Directional responses of vertical arrays show that the two field components make important contributions in specific directions, the continuous field in near-vertical directions and the discrete-mode field in near-horizontal directions. Thus in most conditions neither component can be neglected in predicting array response: the continuous field (usually neglected in long-range propagation calculations) plays an important role, increasingly so in high-loss situations, whereas the discrete-mode field dominates in low-loss cases. Consequently, for a hard-bottom, high array responses are found within ±30° of the horizontal. This is the most striking difference between the array response results for shallow-water and those for an infinitely deep ocean, which show noise arriving mainly from vertically upward directions. For softer bottom types this effect is reduced, but is still evident, particularly when the parameter $m = 1$. Arrivals from near vertically downward, due to bottom-reflected paths at higher than the critical angles, are also characteristic of the array-response patterns in shallow water.

The effect of increasing the source-directionality parameter m is to cause greater bottom interaction and hence more attenuation of the discrete modes in particular. Thus, for soft bottom types, as m increases to 2 or 3 the array-response pattern approaches the 'deep water' result.

Changes in sound-speed profile affect the results to a lesser extent than source directionality; omnidirectional levels increase by 1 to 2 dB in winter conditions and a larger broadside null occurs in summer because lower-order modes are not excited by the shallow source layer.

Comparison of the exact shallow-water results with approximate array responses obtained using a one-dimensional correlation function, under the assumption that the field is homogeneous, shows that the latter method can give large errors in many cases. These occur in low-noise directions, in conditions where the sound-speed profile varies significantly over the array, and where the discrete-mode component of the field is dominant.

It is planned to use SACLANTCEN's new vertical array to acquire wind-noise data in shallow-water areas so as to verify the environmental effects discussed in this report, and also to establish suitable values of the source-directionality parameter, m, for a range of wind speeds and frequencies.

ACKNOWLEDGMENT

The following SACLANTCEN personnel contributed to the work reported:

Ambient-Noise Group	R.M. Heitmeyer	- Helpful technical discussions and reviews of the text.

REFERENCES.

1. WENZ, G.M. Acoustic ambient noise in the ocean: spectra and sources. Journal of the Acoustical Society of America, 34, 1962: 1936-1956.

2. PIGGOTT, C.L. Ambient sea noise at low frequencies in shallow water of the Scotian Shelf. Journal of the Acoustical Society of America, 36, 1964: 2152-2163.

3. CRON, B.F. and SHERMAN, C.H. Spatial-correlation functions for various noise models. Journal of the Acoustical Society of America, 34, 1962: 1732-1736.

4. LIGGETT, W.S., Jr. and JACOBSON, M.J. Covariance of surface-generated noise in a deep ocean. Journal of the Acoustical Society of America, 38, 1965: 303-312.

5. LINETTE, H.M. and THOMPSON, R.J. Directivity study of the noise field in the ocean, employing a correlative dipole. Journal of the Acoustical Society of America, 36, 1964: 1788-1794.

6. TALHAM, R.J. Ambient-sea-noise model. Journal of the Acoustical Society of America, 36, 1964: 1541-1544.

7. STOCKHAUSEN, J.H. Ambient noise vertical directionality - a useful empirical model. Ambient noise vertical directionality - a numerical model. Journal of the Acoustical Society of America, 58, 1975: S121 FFF6 & FFF7.

8. KUPERMAN, W.A. and INGENITO, F. Spatial correlation of surface generated noise in a stratified ocean. Journal of the Acoustical Society of America, 67, 1980: 1988-1996.

9. FRANZ, G.J. Splashes as sources of sound in liquids. Journal of the Acoustical Society of America, 31, 1959: 1080-1096.

10 WILSON, J.H. Low-frequency wind-generated noise produced by the impact of spray with the ocean's surface. Journal of the Acoustical Society of America, 68, 1980: 952-956.

11. KERMAN, B.R. Underwater sound generation by breaking wind waves. Journal of the Acoustical Society of America, 75, 1984: 149-165.

12. URICK, R.J. Principles of Underwater Sound, 2nd edition, New York, N.Y., McGraw-Hill, 1975.

13. ARASE, E.M. and ARASE, T. Correlation of ambient sea noise. Journal of the Acoustical Society of America, 40, 1966: 205-210.

14. AXELROD, E.H., SCHOOMER, B.A. and Von WINKLE, W.A. Vertical directionality of ambient noise in the deep ocean at a site near Bermuda. Journal of the Acoustical Society of America, 37, 1965: 77-83.

15. WOLF, S.N. and INGENITO, F. Site dependence of wind-dominated ambient noise in shallow water. In: WAGSTAFF, R.A. and BLUY, O.Z., eds. Underwater ambient noise. Proceedings of a conference held at SACLANTCEN on 11-14 May 1982, SACLANTCEN CP-32, Part 2. La Spezia, Italy, SACLANT ASW Research Centre, 1982: 22-1 to 22-9.

16. FERLA, M.C. and KUPERMAN, W.A. Wind-generated noise in shallow water, SACLANTCEN SR-79. La Spezia, Italy, SACLANT ASW Research Centre, 1984. [AD A 141 981]

17. JENSEN, F. and FERLA, M.C. SNAP: The SACLANTCEN normal-mode acoustic propagation model, SACLANTCEN SM-121. La Spezia, Italy, SACLANT ASW Research Centre, 1979. [AD A 067 256].

18. DI NAPOLI, F.R. Fast field program for multilayered media, NUSC Report 4103. Newport, R.I., Naval Underwater Systems Center, 1971.

19. KUTSCHALE, H.W. Rapid computation by wave theory of propagation loss in the Arctic Ocean, TR CU-8-73. Palisades, N.Y., Columbia University, Lamont Geological Observatory, 1973.

20. INGENITO, F. Private Communication.

21. JENSEN, F.B. Comparison of transmission loss data for different shallow-water areas with theoretical results provided by a three-fluid normal mode propagation models. In: HASTRUP, O.F. and OLESEN, O.V., eds. Sound propagation in shallow water, proceedings of a conference held at SACLANTCEN on 23-27 September, 1974, II: unclassified papers, SACLANTCEN CP-14. La Spezia, Italy, SACLANT ASW Research Centre, 1974: 79-92. [AD A 004 805]

22. JENSEN, F.B. and KUPERMAN, W.A. Environmental acoustic modelling at SACLANTCEN, SACLANTCEN SR-34. La Spezia, Italy, SACLANT ASW Research Centre, 1979. [AD A 081 853].

23. FERLA, M.C. Modelling of sound propagation losses in the Strait of Sicily and comparison with experimental data, SACLANTCEN SR-52, NATO CONFIDENTIAL. La Spezia, Italy, SACLANT ASW Research Centre, 1981. [AD C 951 259].

APPENDICES

APPENDIX A

EXTENSION TO THE NOISE CORRELATION MODEL FOR SOURCES HAVING PRESSURE RADIATION DIRECTIONALITIES OF THE FORM $\cos^m\alpha$, $m>1$

The basic formula derived by Kuperman and Ingenito for the spatial correlation function between two points a distance R apart at depths z_1 and z_2 is given by Eq. 12 of <A1> as:

$$C(R,z_1,z_2) = 2\pi q^2 \int N(\bar{\rho})\, d\bar{\rho} \int_0^\infty g(n,z_1,z')\, g^*(n,z_2,z')\, J_0(n\,|\,\bar{R} - \bar{\rho}\,|)\, n\, dn \ , \qquad \text{(Eq. A1)}$$

where q = source strength

$N(\rho)$ = source correlation function between sources separated by distance $|\,\bar{\rho}\,|$

z' = depth of source layer

and g is related to the Green's function (see Eq. 8 <A1>).

Liggett and Jacobson <A2> have shown that the source correlation function can be expressed as

$$N(\rho) = 2^m\, m!\, J_m(k\rho)/(k\rho)^m \ , \qquad \text{(Eq. A2)}$$

where k = wave number (at the depth of the source layer),

for sources having pressure radiation directionalities of the form $\cos^m\alpha$ (m not necessarily an integer), where α is measured from the downward vertical.

In <A1> the derivation of C is continued with $N(\rho)$ set equal to $\frac{2}{k^2}\frac{\delta(\rho)}{\rho}$ which corresponds to uncorrelated sources (or sources having directionalities of the form $\cos\alpha$, i.e. the $m = 1$ case).

Here we continue with the general m case and substitute Eq. A2 into Eq. A1 to give

$$C = 2\pi q^2 \int_0^{2\pi} d\phi \int_0^{\infty} \rho\, d\rho\; 2^m m! \frac{J_m(k\rho)}{(k\rho)^m} \int_0^{\infty} J_0(n\,|\bar{R}-\bar{\rho}|)\, g(n,z_1,z')\, g^*(n,z_2,z')\, n\, dn\ ,$$

where ϕ is the angular part of the vector $\bar{\rho}$.

The integral with respect to vector $\bar{\rho}$ can be written (see <A3>)

$$\int_0^{\infty} \rho\, d\rho\, \frac{J_m(k\rho)}{(k\rho)^m} \int_0^{2\pi} J_0\left[n\sqrt{(R^2+\rho^2-2R\rho\cos\phi)}\right] d\phi$$

$$= \int_0^{\infty} \rho\, d\rho\, \frac{J_m(k\rho)}{(k\rho)^m} \int_0^{2\pi} \left[J_0(nR)\, J_0(n\rho) + 2\sum_{r=1}^{\infty} J_r(nR)\, J_r(n\rho)\cos r\phi\right] d\phi$$

The terms involving $\cos r\phi$ are zero when integrated over 2π, leaving the result

$$2\pi\, J_0(nR) \int_0^{\infty} \frac{J_m(k\rho)}{(k\rho)^m} J_0(n\rho)\, \rho\, d\rho$$

This is a standard integral given in <A4> as

$$\int_0^{\infty} J_m(k\rho)\, J_0(n\rho)\, \rho^{1-m}\, d\rho = 0 \qquad \text{for } k < n$$

$$= \left(\frac{k^2-n^2}{2}\right)^{m-1} \frac{k^{-m}}{\Gamma(m)} \qquad \text{for } k > n\ ,$$

which is valid for $\mathrm{Re}(m)>0$, i.e. not necessarily an integer.

Hence the equation for C becomes

$$C = \frac{8m}{k^{-m}}\pi^2\, q^2 \int_0^{k} J_0(nR)\, g(n,z_1,z')\, g^*(n,z_2,z')(k^2-n^2)^{m-1}\, n\, dn \qquad \text{(Eq. A3)}$$

In Sect. II of <A1>, the case of a noise field of discrete normal modes is dealt with by substitution of the appropriate function g in terms of the modal eigenfunctions, u_n. This results in Eq. 26 of <A1> as

$$C = \frac{iq^2}{4} \int N(\bar{\rho})\, d\bar{\rho} \sum_{n,p} u_n(z')\, u_p(z')\, u_n(z_1)\, u_p(z_2)\, f_{np}$$

$$\cdot \left[H_0^{(1)}(k_n \left| \bar{R}-\bar{\rho} \right|) - H_0^{(1)}\, (-k_p^* \left| \bar{R}-\bar{\rho} \right|)\right] , \quad \text{(Eq. A4)}$$

where k_n = wave number of nth mode

and

$$f_{np} = \frac{1}{k_n^2 - k_p^2} \quad , \qquad n = p$$

$$= \frac{1}{4i\alpha_n K_n} \quad , \qquad n = p$$

where K_n and α_n are the real and imaginary parts of k_n.

Substitution of Eq. A2 for the general form of $N(\rho)$ leads to the following integral over ρ:

$$\int_0^\infty 2^m\, m!\, \frac{J_n(k\rho)}{(k\rho)^m}\, \rho\, d\rho \left\{ \int_0^{2\pi} H_0^{(1)} \left[k_n \sqrt{(R^2 + \rho^2 - 2R\rho\, \cos\phi)} \right] d\phi \right.$$

$$\left. + \int_0^{2\pi} H_0^{(1)} \left[k_p^* \left(\sqrt{R^2 + \rho^2 - 2R\rho\, \cos\phi}\right) \right] d\phi \right\}$$

The integrals with respect to ϕ can be evaluated as before leaving

$$\int_0^\infty 2^m\, m!\, \frac{J_m(k\rho)}{(k\rho)^m}\, \rho\, d\rho \left[2\pi\, J_0(k_n R)\, J_0(k_n \rho) + 2\pi\, J_0(k_p R)\, J_0(k_p \rho) \right.$$

$$\left. + 2\pi i \begin{cases} Y_0(k_n R)\, J_0(k_n \rho) - Y_0(k_p R)\, J_0(k_p \rho) , & \rho < R \\ Y_0(k_n \rho)\, J_0(k_n R) - Y_0(k_p \rho)\, J_0(k_p R) , & \rho > R \end{cases} \right] \quad \text{(Eq. A5)}$$

For the diagonal terms only of the mode summation of Eq. A4, we have n=p and obtain for the correlation function

$$C^{diag} = iq^2 2^m m! \pi \int_0^\infty \frac{J_m(k\rho)}{(k\rho)^m} J_0(k_n R)\, J_0(k_n\rho) \sum_n u_n^2(z')\, u_n(z_1)\, u_n(z_2)\, f_{nn}\, \rho\, d\rho$$

This integral can be evaluated (see <A4>) to give

$$C^{diag} \begin{cases} = \dfrac{iq^2}{k^2}\, 2\pi m \sum_n u_n^2(z')\, u_n(z_1)\, u_n(z_2)\, f_{nn}\, J_0(k_n R) \left(\dfrac{k^2 - K_n^2}{k^2}\right)^{m-1} \\ \qquad\qquad\qquad\qquad\qquad\qquad\qquad\qquad\qquad\qquad \text{for } K_n < k, \\ = 0 \quad \text{otherwise.} \end{cases}$$

(Eq. A6)

This function is the result for the incoherent combination of the normal modes and is totally real (see form of f_{nm} for n=m). The extra terms that account for the phase differences between modes involve the remaining integrals of Eq. A5 containing the Bessel function of the second kind, Y_0.

These integrals are

$$Y_0(k_n R) \int_0^R \frac{J_m(k\rho)}{(k\rho)^m} J_0(k_n\rho)\, \rho\, d\rho - Y_0(k_p R) \int_0^R \frac{J_m(k\rho)}{(k\rho)^m} J_0(k_p\rho)\, \rho\, d\rho$$

and

$$J_0(k_n R) \int_R^\infty \frac{J_m(k\rho)}{(k\rho)_m} Y_0(k_n\rho)\, \rho\, d\rho - J_0(k_p R) \int_R^\infty \frac{J_m(k\rho)}{(k\rho)^m} Y_0(k_p\rho)\, \rho\, d\rho \quad .$$

It appears impossible to evaluate these integrals analytically.

However, studies with the computer model constructed for the m = 1 case of <A1>, which contains both coherent and incoherent mode summation options, have shown little difference between the two for noise intensity

and array response at the frequencies of interest. As an example, Fig. A1 shows the array response to a discrete-mode field, the solid curve being for coherent and the dashed curve for incoherent mode summations. These results are for 480 Hz, isovelocity profile and soft (S.E. Elba) bottom conditions, and show the largest difference between the two calculations of all the sets of conditions used in the main text. As we see, the difference is almost negligible. Thus the incoherent result of Eq. A6 for $m > 1$ has been added to the computer code for noise intensity and correlation coefficient calculations. All results reported in the main text, for both $m = 1$ and $m > 1$, were obtained by incoherent mode combination.

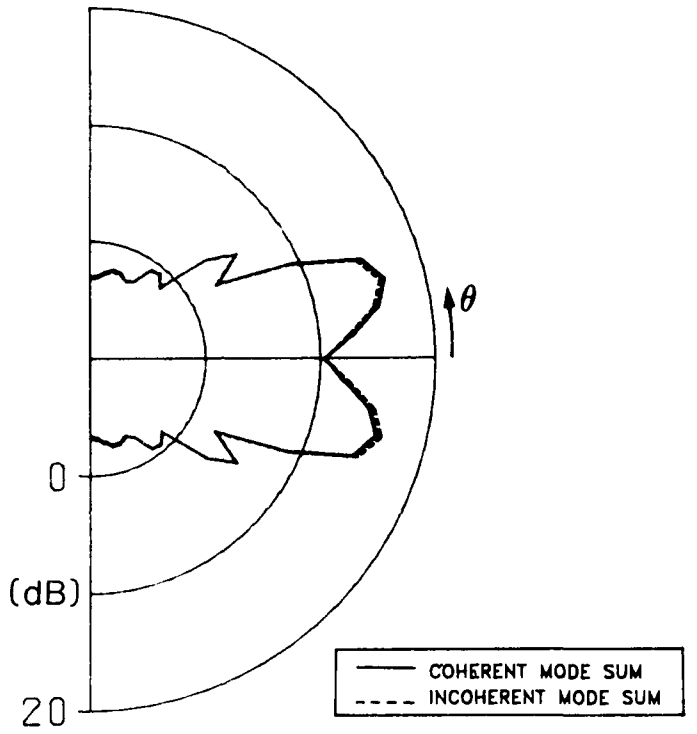

FIG. A1 VERTICAL ARRAY RESPONSE TO THE DISCRETE MODE FIELD AT 480 Hz IN ISOVELOCITY/SOFT BOTTOM CONDITIONS, WITH m = 1 OBTAINED BY SUMMING THE MODE CONTRIBUTIONS COHERENTLY (solid curve) AND INCOHERENTLY (dashed curve).

REFERENCES

A1 KUPERMAN, W.A. and INGENITO, F. Spatial correlation of surface generated noise in a stratified ocean. Journal of the Acoustical Society of America, 67, 1980: 1988-1996.

A2 LIGGETT, W.S., Jr. and JACOBSON, M.J. Covariance of surface-generated noise in a deep ocean. Journal of the Acoustical Society of America, 38, 1965: 303-312.

A3 TRANTER, C.J. Bessel Functions with some Physical Applications, London, Hodder/English Universities Press, 1968.

A4 WATSON, G.N. A treatise on the Theory of Bessel Functions", 2nd edition, Cambridge, U.K., Cambridge University Press, 1966: p. 415

APPENDIX B

EXAMPLES OF MODELLED NOISE INTENSITIES AS A FUNCTION OF DEPTH

This appendix contains results for noise intensity (relative to unit source level) vs depth, obtained using different bottom types and sound-speed profiles in the shallow-water noise model. Figure B1 gives the 150 Hz intensities plotted over the 100 m water column for the hardest bottom of the three types defined in Ch. 2 of the main text. These correspond to an isovelocity sound-speed profile and show the total field (solid lines) and the discrete-mode field (dashed lines) for source-pressure directionalities of $\cos\alpha$ (i.e., m = 1) and $\cos^2\alpha$ (i.e., m = 2). Noise levels are significantly different for these two cases, and the difference between the discrete-mode field and the total field increases for higher source directionality. The variation with depth however is not very large, generally within 1 to 2 dB between depths of 20 m and 80 m, with higher oscillations near the boundaries.

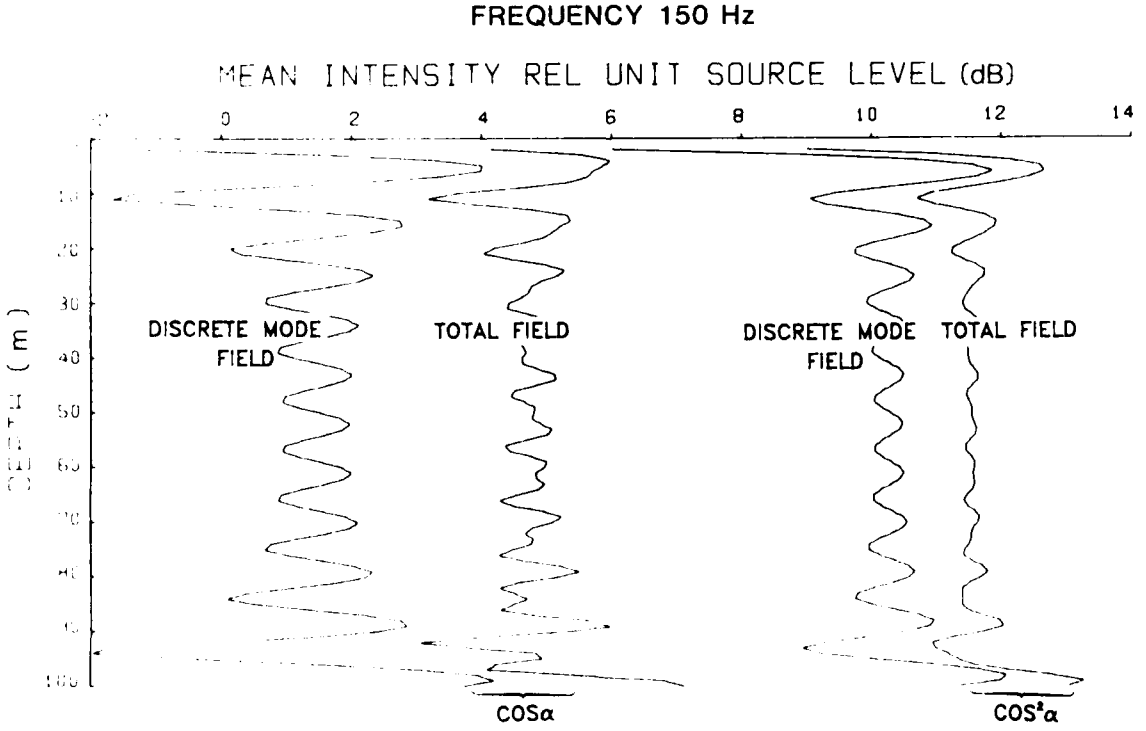

FIG. B1 NOISE INTENSITY (relative to unit source level) vs DEPTH FOR 150 Hz, ISOVELOCITY PROFILE, AND HARD-BOTTOM CONDITIONS.

Figures B2 and B3 give the total-field results for three bottom types, for an isovelocity and a summer sound-speed profile respectively, both for 150 Hz and $\cos\alpha$ source directionality. The intermediate bottom, though not containing a soft sediment layer, as does the soft bottom, gives rise to the lowest intensities, due to shear losses. The result is about 1 dB less than the soft-bottom noise over most of the water column and 3 to 4 dB less than the hard-bottom noise. The isovelocity results are more vertical than the summer results, and are higher by about 1 dB at depths below the 40 m thermocline of the summer profile for all bottom types.

Noise intensities for 480 Hz are plotted in Fig. B4 for the three bottom types, summer profile, and $\cos\alpha$ (i.e., m = 1) source directionality. For this frequency the Sicily bottom gives rise to marginally higher noise than the S.E. Elba bottom, since the shear losses are reduced. The effect of the sound-speed gradient between 40 and 50 m is evident, but otherwise the depth variation is less than 0.5 dB to within 10 m of the surface or bottom. The results for both frequencies indicate that the vertical inhomogeneity of shallow water wind noise must be due more to phase variations with depth than to amplitude variations with depth.

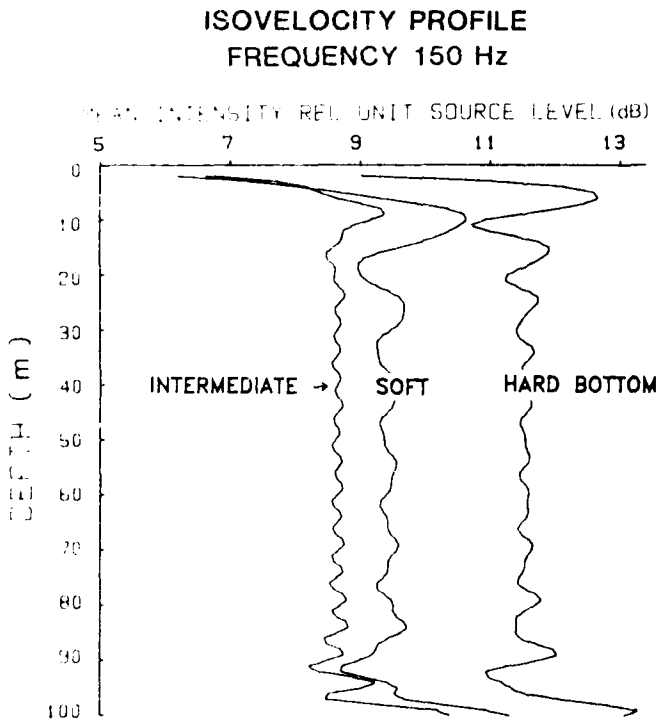

FIG. B2 NOISE INTENSITY (relative to unit source level) vs DEPTH FOR 150 Hz, ISOVELOCITY PROFILE, AND THREE BOTTOM TYPES.

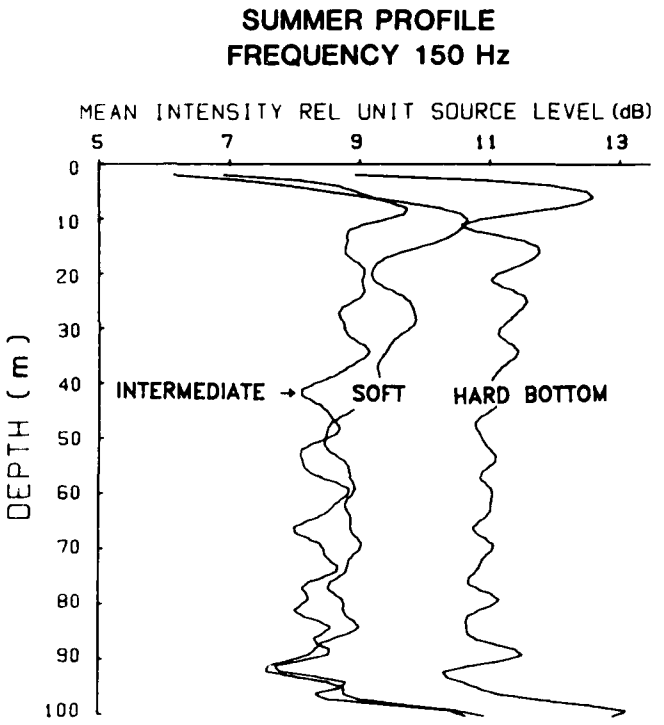

FIG. B3 NOISE INTENSITY (relative to unit source level) vs DEPTH FOR 150 Hz, SUMMER PROFILE, AND THREE BOTTOM TYPES.

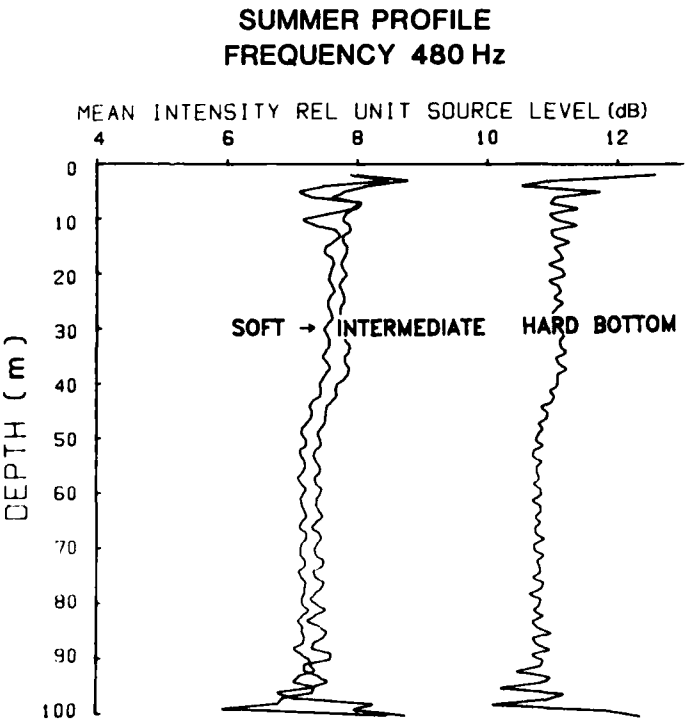

FIG. B4 NOISE INTENSITY (relative to unit source level) vs DEPTH FOR 480 Hz, SUMMER PROFILE, AND THREE BOTTOM TYPES.

APPENDIX C

THE ARRAY-RESPONSE EQUATION

The noise power output, P, of an array of N hydrophones can be written in matrix form, see <C1>, as

$$P = \underline{W}^{*T}\,\underline{C}\,\underline{W} \quad , \qquad \text{(Eq. C1)}$$

where $\underline{W}$ is the column vector of the N complex hydrophone weightings, $w_n e^{i\phi_n}$

and $\underline{C}$ is the (NxN) Hermitian matrix of complex correlation coefficients.

(^{*T} denotes conjugate transpose).

Thus

w_n = amplitude weighting of the nth hydrophone.

ϕ_n = phase weighting of the nth hydrophone,

and

c_{np} = complex correlation coefficient between the nth and pth hydrophone.

In this report we are concerned with the directional response of uniform equally spaced line arrays, and so we have

w_n = 1 for all n,

and

$\phi_n = 2\pi nd \sin\theta/\lambda$,

where

d = hydrophone spacing

λ = wavelength

and

θ = steered direction from broadside, in the plane of the array.

For a homogeneous noise field, such as that assumed by the Cron and Sherman model <C2>, the matrix [C] is of Toeplitz form and only (N-1) unique correlation coefficients need to be calculated, (see Appendix D for the appropriate equations of Cron and Sherman). For the inhomogeneous shallow-water field [C] is not of Toeplitz form and contains N(N-1)/2 unique complex coefficients. This matrix is calculated by the shallow-water model when hydrophone positions are specified, and is used in Eq. C1 to obtain P(0) for different environmental conditions, as presented in Sects. 2.2 and 2.3 of the main text. The extent of the inhomogeneity is considered in Sect. 2.4, by calculating P(0) using Toeplitz matrices for [C] constructed from either the first row or the last column of the full matrix produced by the model.

REFERENCE

C1 EDELBLUTE, D.J., FISK, J.M. and KINNISAN, G.L. 'Criteria for optimum-signal-detection theory for arrays'. Journal of the Acoustical Society, 41, 1966: 199-205.

C2 CRON, B.F. and SHERMAN, C.H. Spatial correlation functions for various noise models. Journal of the Acoustical Society of America, 34, 1962: 1732-1736.

APPENDIX D

THE CRON AND SHERMAN MODEL FOR INFINITELY DEEP WATER

Cron and Sherman <D1> derived formulae for the real parts of the correlation coefficient between vertically and horizontally separated points in a homogenous half-space for source directionality functions $\cos^m\alpha$ (integer m). Kuperman and Ingenito <D2> show that their own results reduce to those of Cron and Sherman for this type of environment. From their equation A13, the imaginary part of the correlation coefficient for vertically spaced points can easily be derived.

For points separated by a vertical spacing d, the normalized complex correlation coefficient, C_v, is given by

$$C_v = 2\,mk^{-2m} \int_0^k x^{2m-1}(\cos xd + i \sin xd)\, dx$$

This integral can be evaluated for a given m; for the m = 1 and m = 2 cases we have the results

$$C_v(m=1) = \frac{2 \sin kd}{kd} + \frac{2(\cos kd - 1)}{(kd)^2} - 2i\left(\frac{\cos kd}{kd} - \frac{\sin kd}{(kd)^2}\right)$$

and

$$C_v(m=2) = \frac{4 \sin kd}{kd} + \frac{12 \cos kd}{(kd)^2} - \frac{24 \sin kd}{(kd)^3} - \frac{24(\cos kd - 1)}{(kd)^4}$$

$$- 4i\left(\frac{\cos kd}{kd} - \frac{3 \sin kd}{(kd)^2} - \frac{6 \cos kd}{(kd)^3} + \frac{6 \sin kd}{(kd)^4}\right)$$

The real parts of the above equations agree with the results of Cron and Sherman. The noise intensity at a single hydrophone due to unit source level can easily be derived from the Cron and Sherman equations as π/m. This level, 10 log (π/m), is a lower bound for noise levels in isovelocity shallow water (discounting volume attenuation and surface-scattering losses), which must be at least as high as infinitely deep water levels.

REFERENCES

D1 CRON, B.F. and SHERMAN, C.H. Spatial correlation functions for various noise models. Journal of the Acoustical Society of America, 34, 1962: 1732-1736.

D2 KUPERMAN, W.A. and INGENITO, F. Spatial correlation of surface generated noise in a stratified ocean. Journal of the Acoustical Society of america, 67, 1980: 1988-1996.

KEYWORDS

AMBIENT NOISE
ANGLE OF INCIDENCE
ARRAY POWER OUTPUT
ARRAY RESPONSE
ATTENUATION
BESSEL FUNCTION
BOTTOM LOSS
BOTTOM
COMPRESSIONAL SPEED
CONTINUOUS MODAL SPECTRUM
CONTINUOUS SPECTRUM
CORRELATION COEFFICIENT
CORRELATION MATRIX
CRITICAL ANGLE
CRON AND SHERMAN MODEL
DEEP WATER
DISCRETE MODE
ELBA
FAST FIELD PROGRAM
FREQUENCY
GRAVITY WAVE
GRAZING ANGLE
GREEN'S FUNCTION
HARD BOTTOM
HOMOGENEOUS SOURCE LAYER
INTERMEDIATE BOTTOM
ISOVELOCITY CONDITIONS
[illegible]
KUPERMAN-INGENITO MODEL
[illegible] PROPAGATION
NEAR FIELD
NOISE
NON-TOEPLITZ MATRIX
NORMAL-MODE PROPAGATION MODEL
PLANE WAVE INCIDENCE
PROPAGATION
SEA STATE
SHALLOW WATER
SHEAR EFFECT
SHEAR WAVE PROPAGATION
SNAP
SOFT BOTTOM
SOUND SPEED PROFILE
SOURCE DIRECTIONALITY
SOUTHWESTERN APPROACHES
SPATIAL CORRELATION FUNCTION
SPATIAL CORRELATION
SPRAY
SPRING
STRAIGHT LINE RAY PROPAGATION
STRAIT OF SICILY

STRATIFIED OCEAN
SUMMER
SWAP
TOEPLITZ MATRIX
VERTICAL ARRAY
VERTICAL FIELD DIRECTIONALITY
VERTICAL LINE ARRAY
VERTICALLY INHOMOGENOUS FIELD
VERTICAL CORRELATION FUNCTION
WAVE THEORY
WHITECAPS
WIND SPEED 10 kn
WIND SPEED 15 kn
WIND SPEED 25 kn
WIND SPEED 40 kn
WIND SPEED 50 kn
WIND
WINTER

FREQUENCIES (Hz)

50
150
200
300
480
500
700
1000
3200

INITIAL DISTRIBUTION

MINISTRIES OF DEFENCE	Copies
JSPHQ Belgium	2
DND Canada	10
CHOD Denmark	8
MOD France	8
MOD Germany	15
MOD Greece	11
MOD Italy	10
MOD Netherlands	12
CHOD Norway	10
MOD Portugal	2
MOD Spain	2
MOD Turkey	5
MOD U.K.	20
SECDEF U.S.	68

NATO AUTHORITIES	Copies
Defence Planning Committee	3
NAMILCOM	2
SACLANT	10
SACLANTREPEUR	1
CINCWESTLANT/COMOCEANLANT	1
COMSTRIKFLTANT	1
COMIBERLANT	1
CINCEASTLANT	1
COMSUBACLANT	1
COMMAIREASTLANT	1
SACEUR	2
CINCNORTH	1
CINCSOUTH	1
COMNAVSOUTH	1
COMSTRIKFORSOUTH	1
COMEDCENT	1
COMMARAIRMED	1
CINCHAN	3

SCNR FOR SACLANTCEN	Copies
SCNR Belgium	1
SCNR Canada	1
SCNR Denmark	1
SCNR Germany	1
SCNR Greece	1
SCNR Italy	1
SCNR Netherlands	1
SCNR Norway	1
SCNR Portugal	1
SCNR Turkey	1
SCNR U.K.	1
SCNR U.S.	2
SECGEN Rep. SCNR	1
NAMILCOM Rep. SCNR	1

NATIONAL LIAISON OFFICERS	
NLO Canada	1
NLO Denmark	1
NLO Germany	1
NLO Italy	1
NLO U.K.	1
NLO U.S.	1

NLR TO SACLANT	
NLR Belgium	1
NLR Canada	1
NLR Denmark	1
NLR Germany	1
NLR Greece	1
NLR Italy	1
NLR Netherlands	1
NLR Norway	1
NLR Portugal	1
NLR Turkey	1
NLR UK	1
NLR US	1

Total initial distribution	249
SACLANTCEN Library	10
Stock	21
Total number of copies	280

END

FILMED

5-85

DTIC